Synthesis of 7-Azaindoles by Chichibabin Cyclization:
Reversible Base-Mediated Dimerization of 3-Picolines

Yun Ma, Sean Breslin, Ivan Keresztes, Emil Lobkovsky and David B. Collum*†

Contribution from the Department of Chemistry and Chemical Biology
Baker Laboratory, Cornell University, Ithaca, New York 14853-1301

Supporting Information

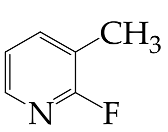

1

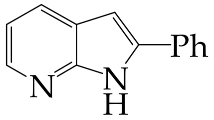

2

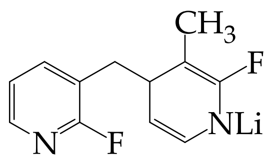

5

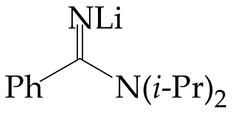

6

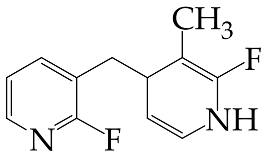

7

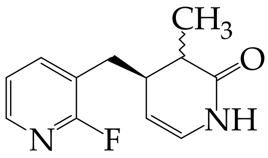

8

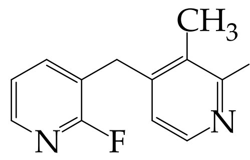

9

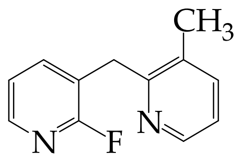

10

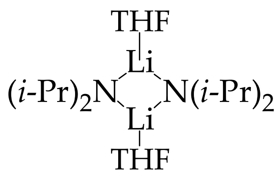

11

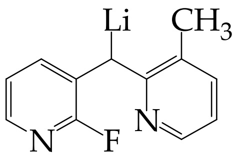

13

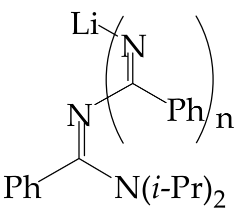

14

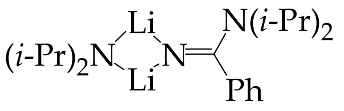

18

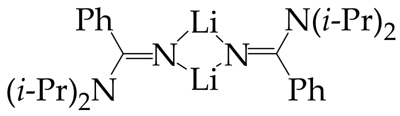

19

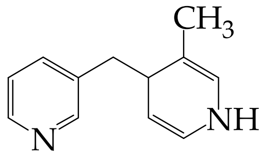

23

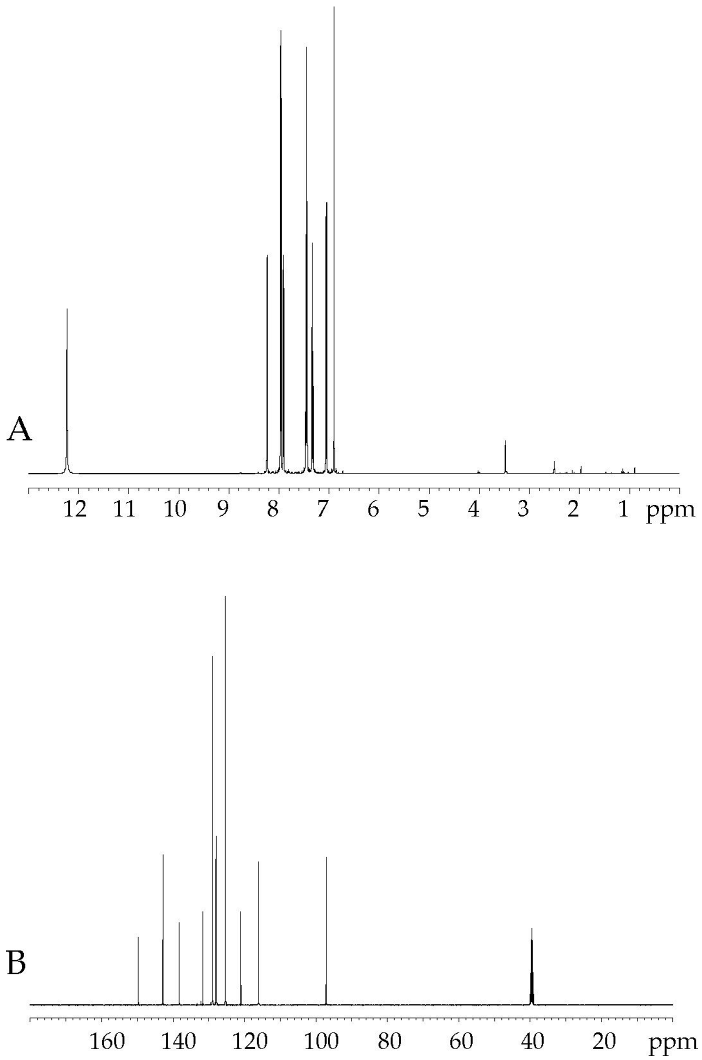

I. NMR spectra of **2** in DMSO-d_6: (**A**) ^{1}H NMR; and (**B**) ^{13}C NMR.

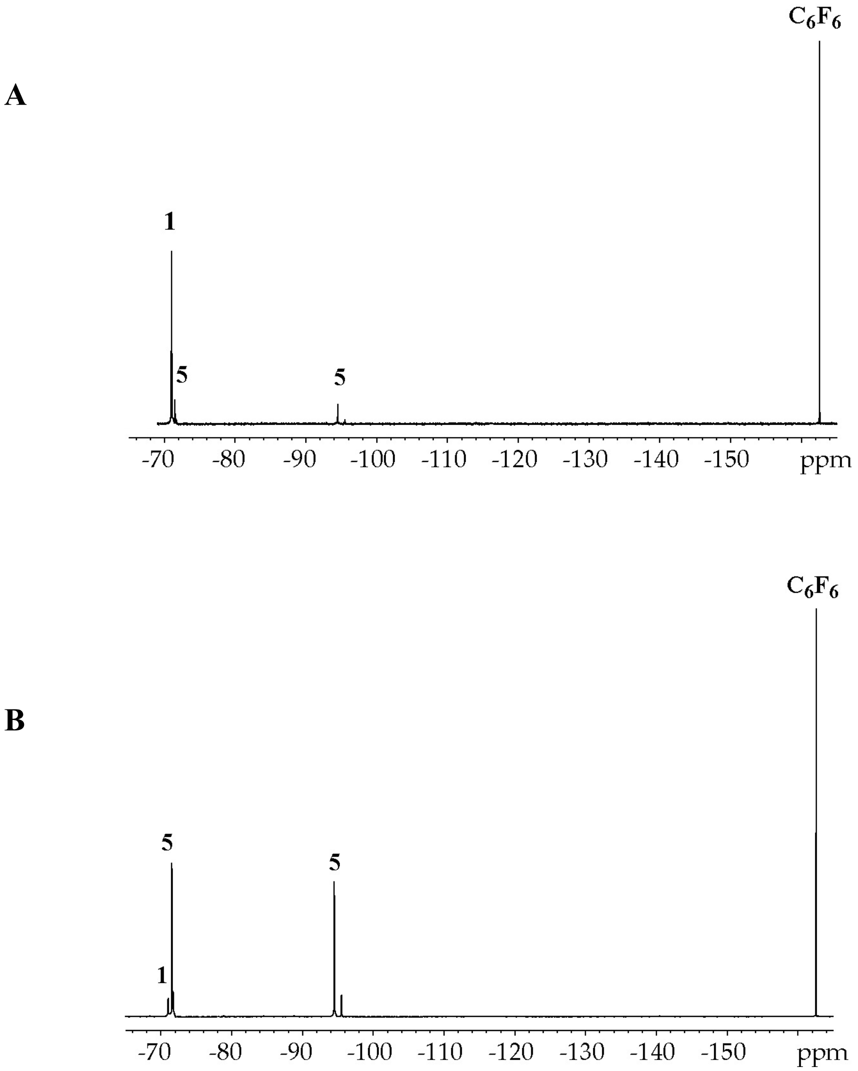

II. ^{19}F NMR spectra of 0.10 M **1** with 0.10 M LDA in neat THF at –78 ºC showing reaction to form **5**. Hexafluorobenzene (0.60 M in neat THF) is included as an internal standard in a sealed capillary tube. Spectra were recorded (**A**) after 30 s aging at –40 ºC; and (**B**) after 10 min aging at –40 ºC.

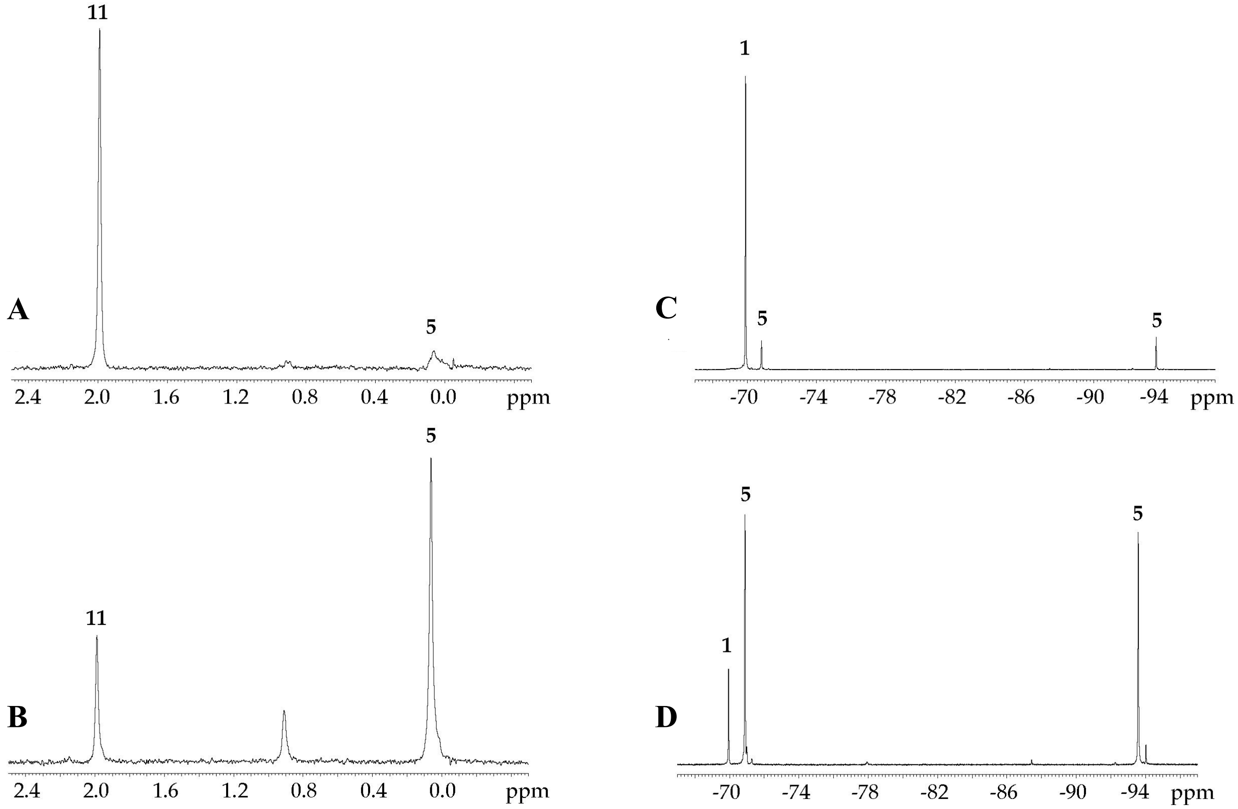

III. ^{6}Li and ^{19}F NMR spectra of 0.30 M **1** with 0.30 M [^{6}Li]LDA in neat THF at –78 ºC showing reaction to form **5**. Spectra were recorded as follows: (**A**) ^{6}Li spectrum at –40 ºC after 10 s aging; **(B**) ^{6}Li spectrum at –40 ºC after 3 min aging; (**C**) ^{19}F spectrum at –40 ºC after 10 s aging; and (**D**) ^{19}F spectrum at –40 ºC after 3 min aging.

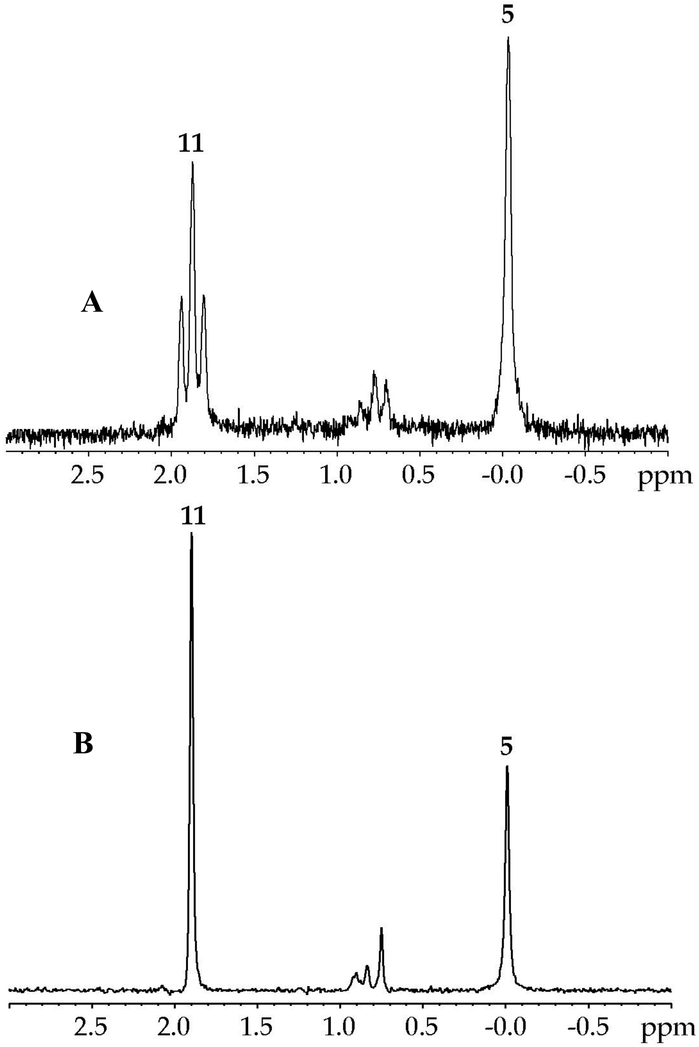

IV. ^{6}Li NMR spectra of 0.30 M **1** with 0.30 M [^{6}Li,^{15}N]LDA in neat THF recorded at –78 ºC after aging at -55 ºC for 1 h showing no ^{6}Li-^{15}N coupling of **5**. (**A**) ^{6}Li spectrum and (**B**) ^{6}Li{^{15}N}spectrum.

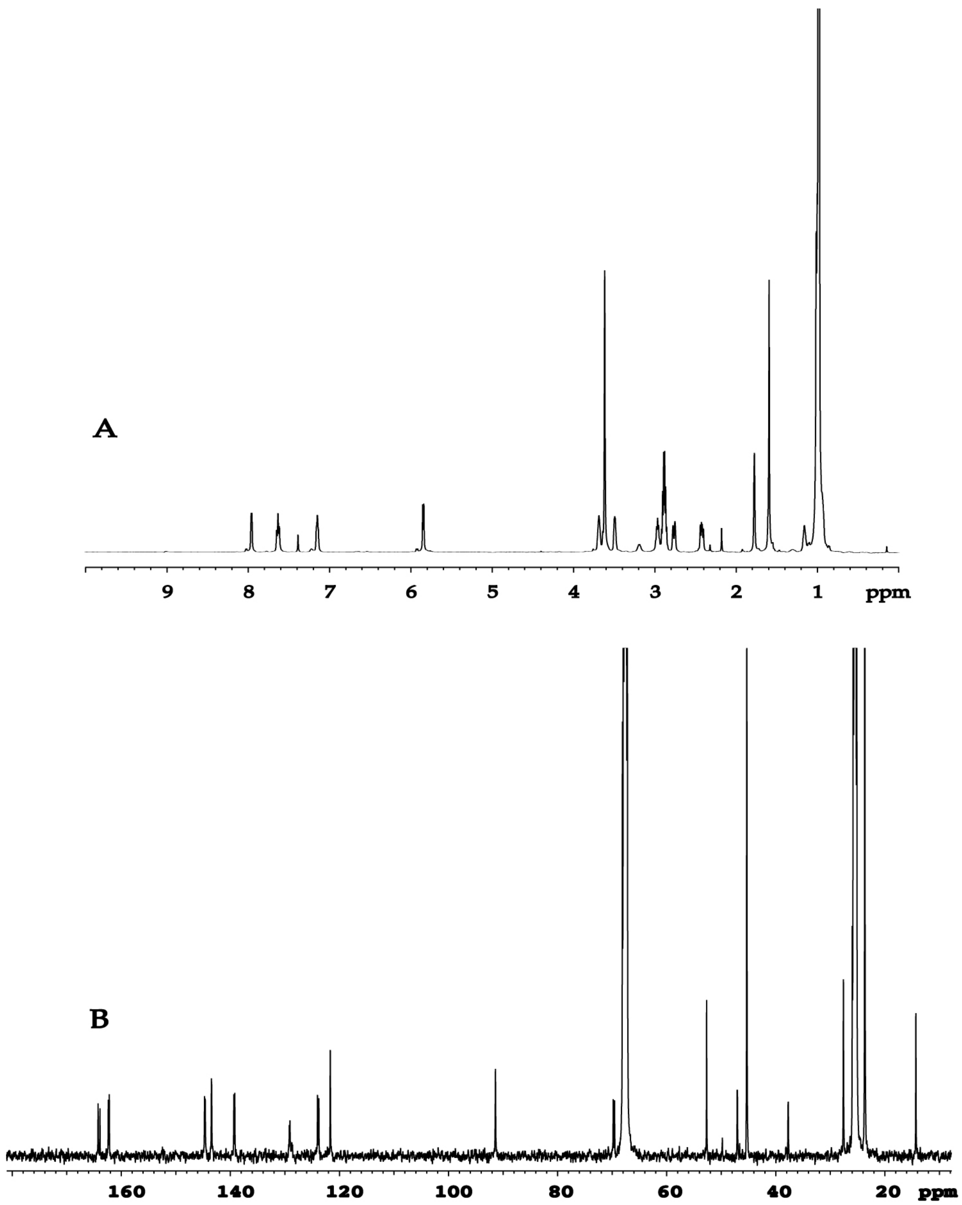

V. ^{1}H NMR spectra of 0.10 M **1** with 0.10 M LDA in neat THF at –78 ºC showing reaction to form **5**. (**A**) ^{1}H NMR spectra were recorded after 30 min aging at –40 ºC; and **(B)** ^{13}C NMR spectra were recorded after 30 min aging at –40 ºC.

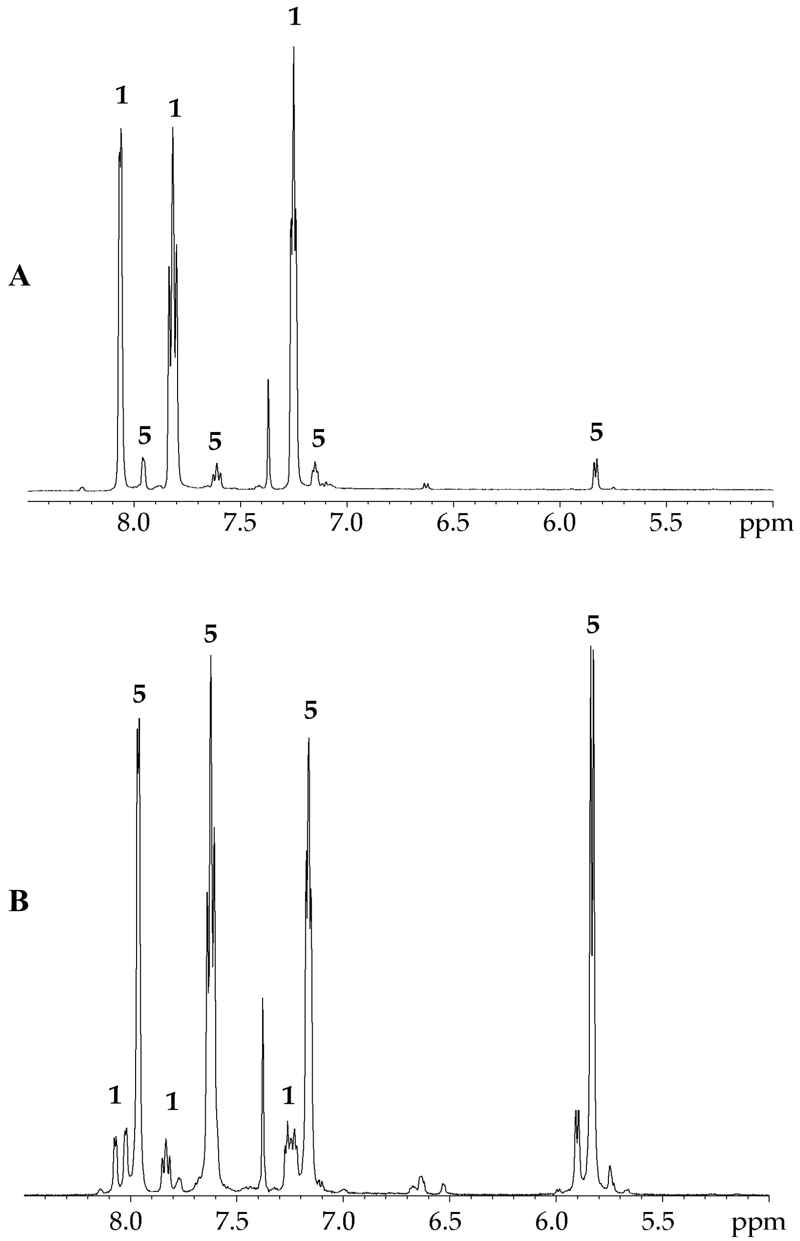

VI. ^{1}H NMR spectra of 0.30 M **1** with 0.30 M LDA in neat THF at –78 ºC showing reaction to form **5**. Only aromatic and vinylic regions are included for clarity. Spectra were recorded (**A**) after 30 s aging at –40 ºC; and (**B**) after 10 min aging at –40 ºC.

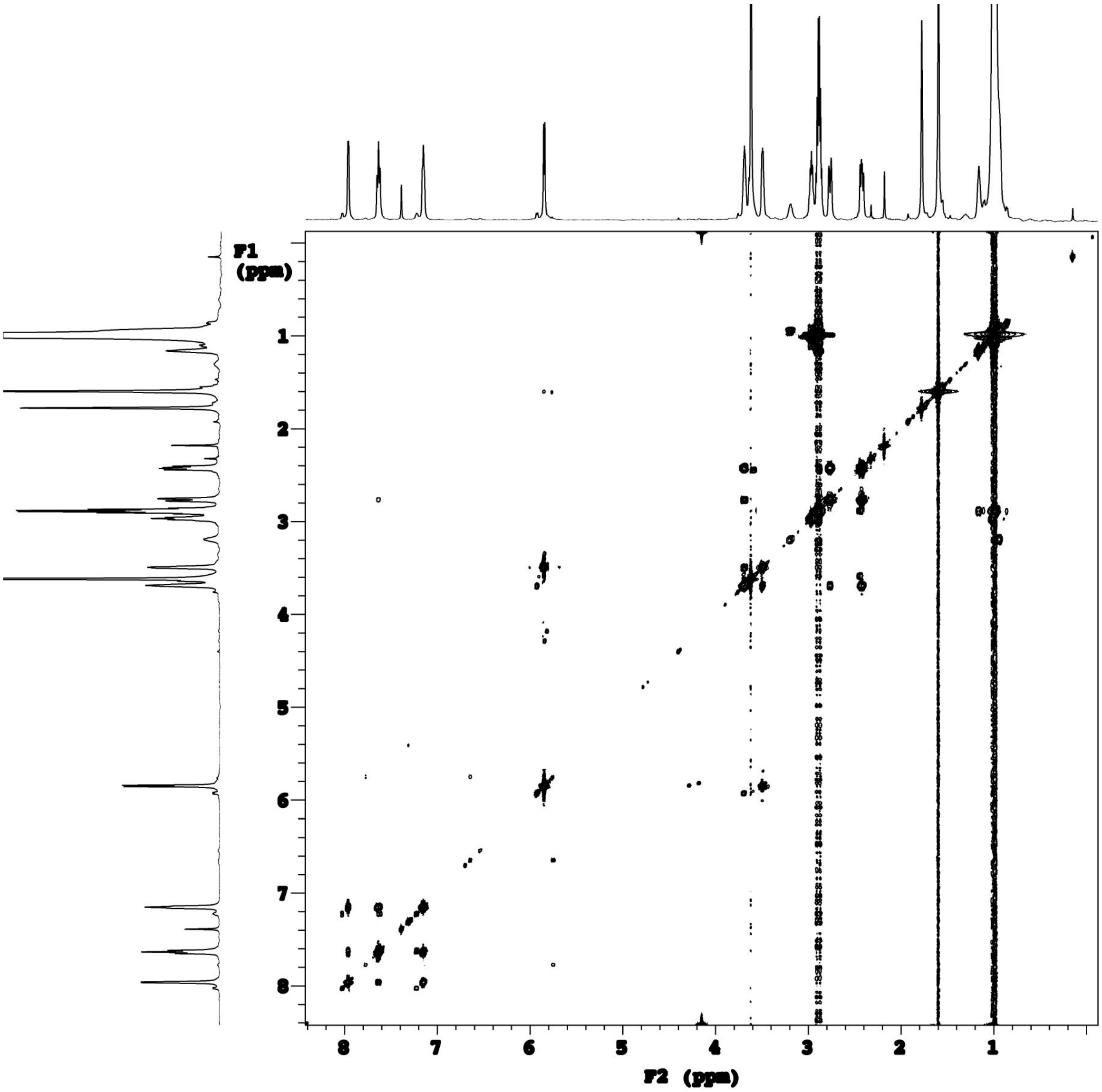

VII. [^{1}H,^{1}H]COSY NMR spectrum of 0.10 M **1** with 0.10 M LDA in neat THF-d_8 at –78 ºC showing reaction to form **5**. The spectrum was recorded after 30 min aging at –40 ºC.

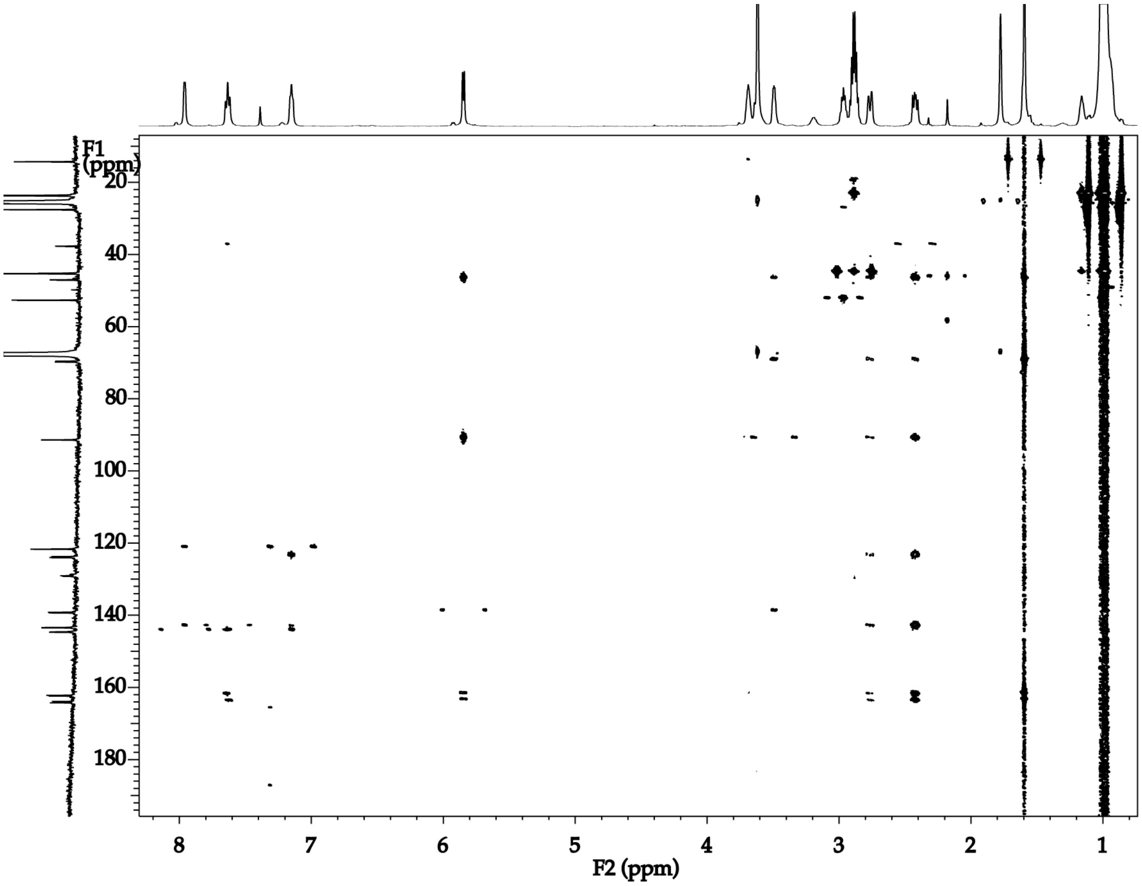

VIII. [^{1}H,^{13}C]HMBC NMR spectrum of **5** revealing long range ^{1}H-^{13}C heteronuclear correlation. The sample was prepared with 0.10 M **1** with 0.10 M LDA in neat THF at –78 ºC . The spectrum was recorded after 30 min aging at –40 ºC.

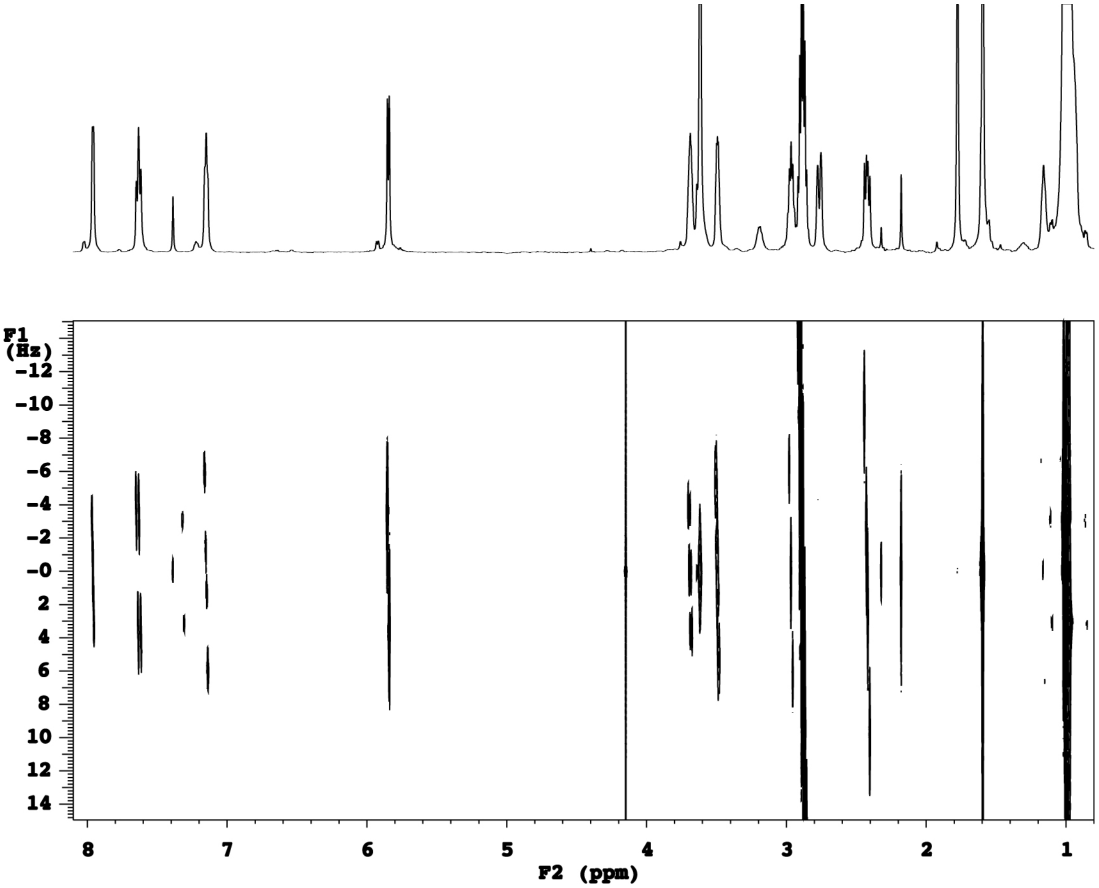

IX. $J\{^{1}H,^{19}F\}$-resolved spectrum of **5** . The sample was prepared with 0.10 M **1** with 0.10 M LDA in neat THF at –78 ºC. The spectrum was recorded after 30 min aging at –40 ºC.

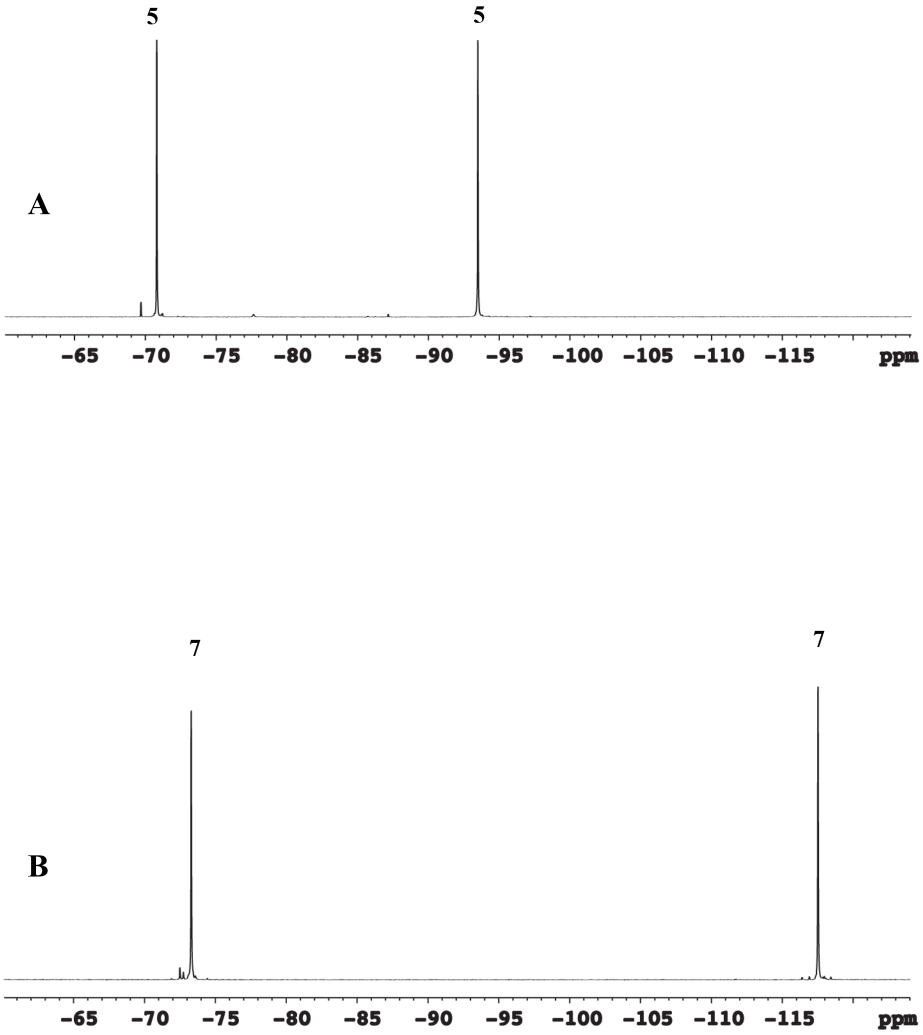

X. ^{19}F NMR spectra: (**A)** after complete reaction of **1** with LDA to form **5** at –40 ºC; and (**B**) immediately after quench of sample with H_2O/THF at –40 ºC to form dihydropyridine **7**.

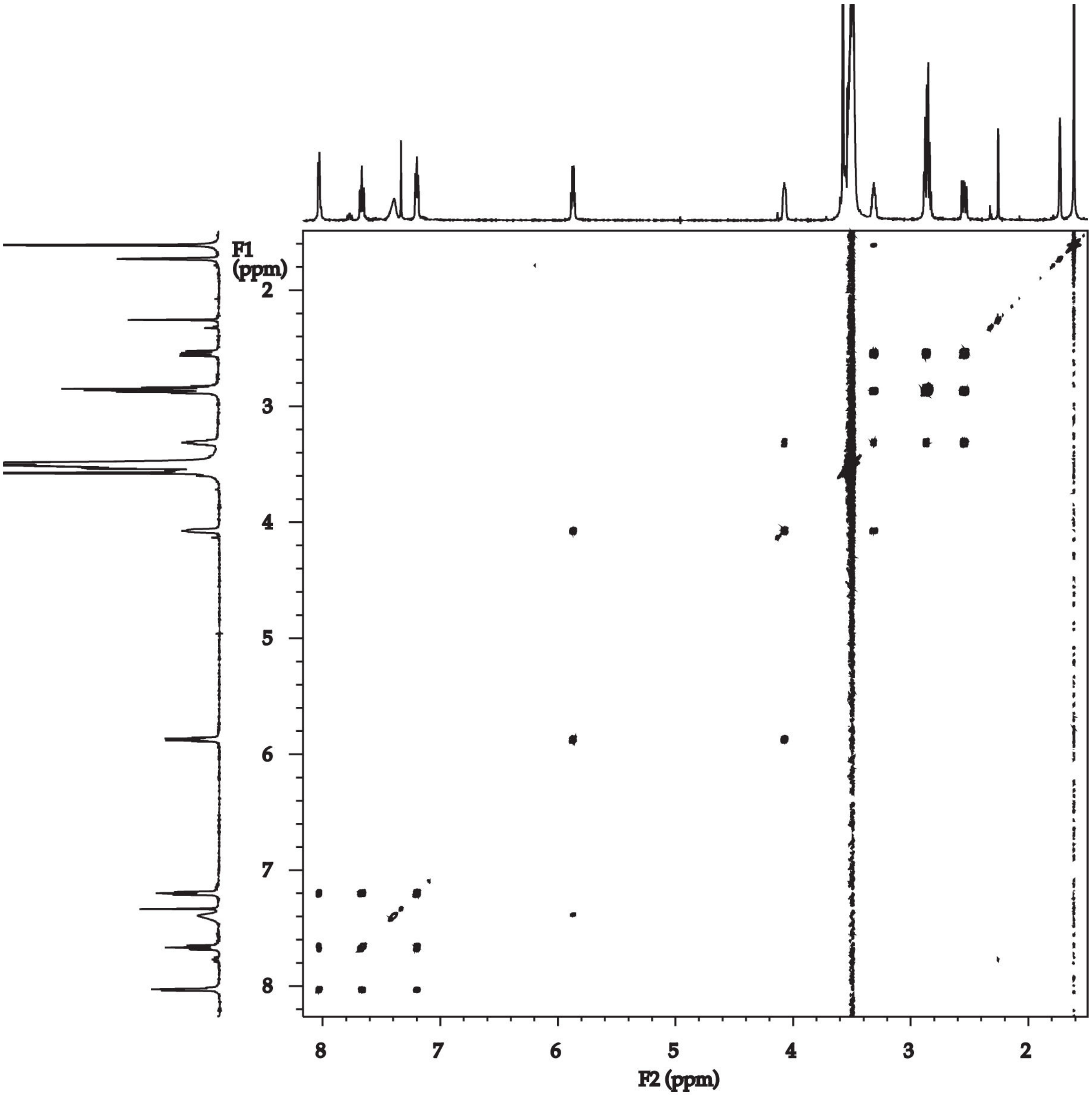

XI. [^{1}H,^{1}H]COSY NMR spectrum of **7** recorded in neat THF-d_8 at –70 ºC.

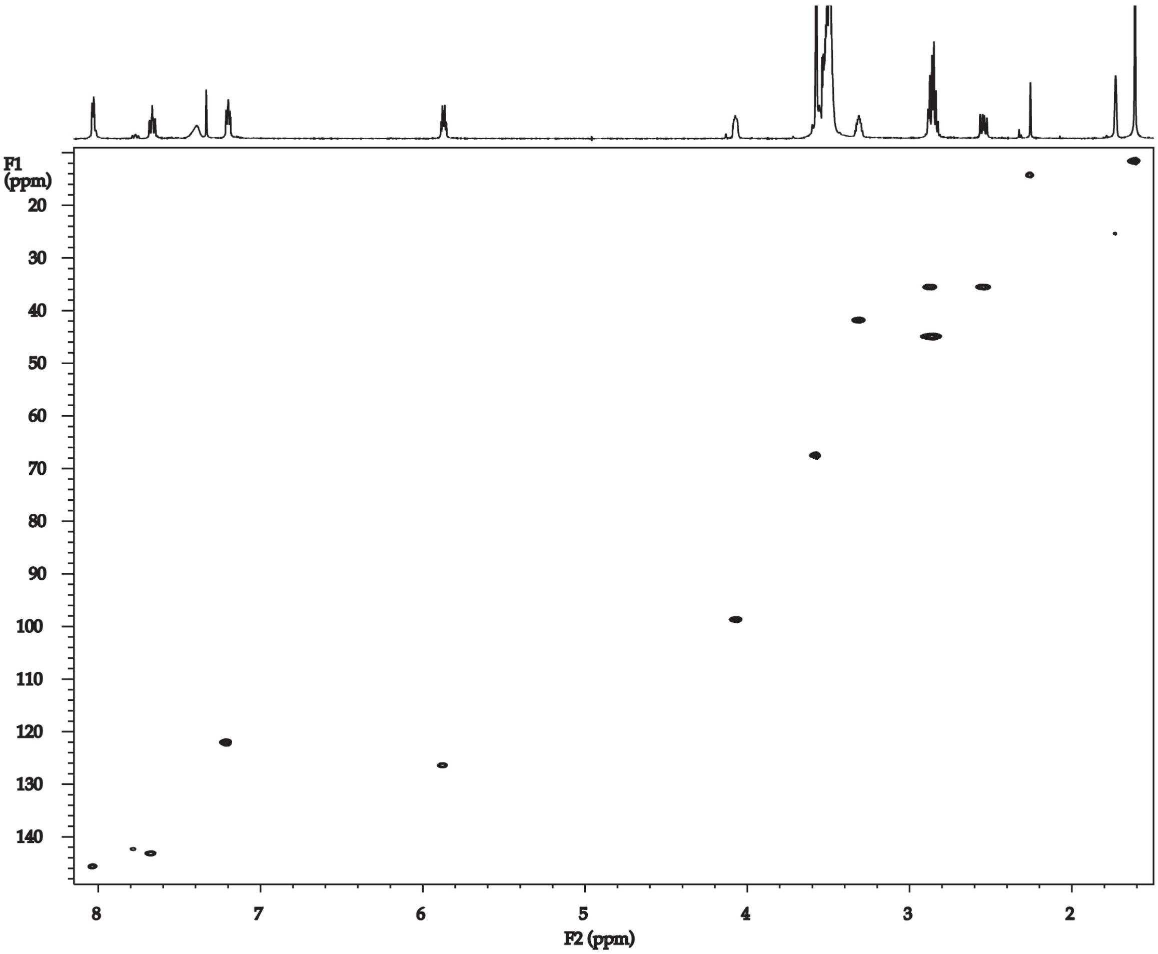

XII. [^{1}H,^{13}C]HSQC NMR spectrum of **7** recorded in neat THF-*d*$_8$ at -70 ºC.

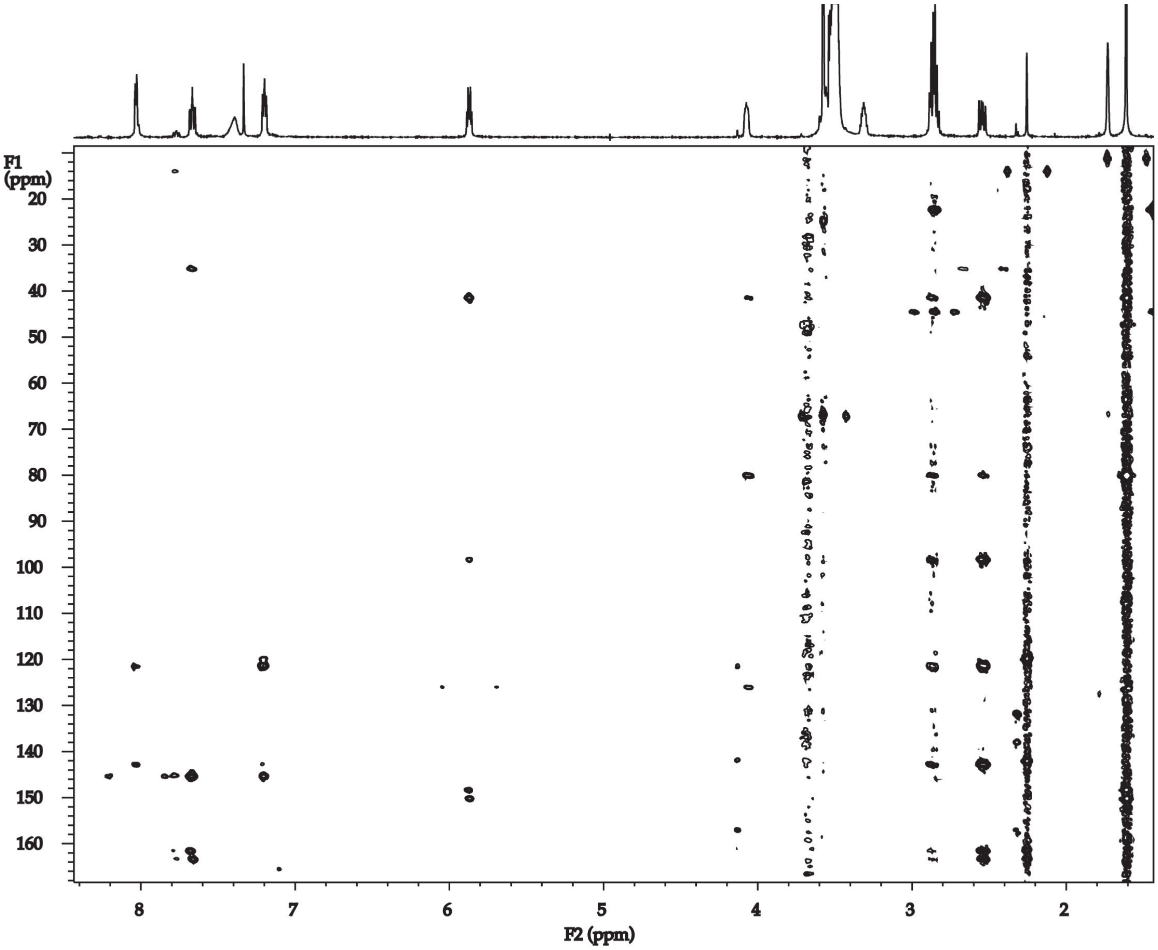

XIII. [^{1}H,^{13}C]HMBC NMR spectrum of **7** recorded in neat THF-d_8 at -70 ºC.

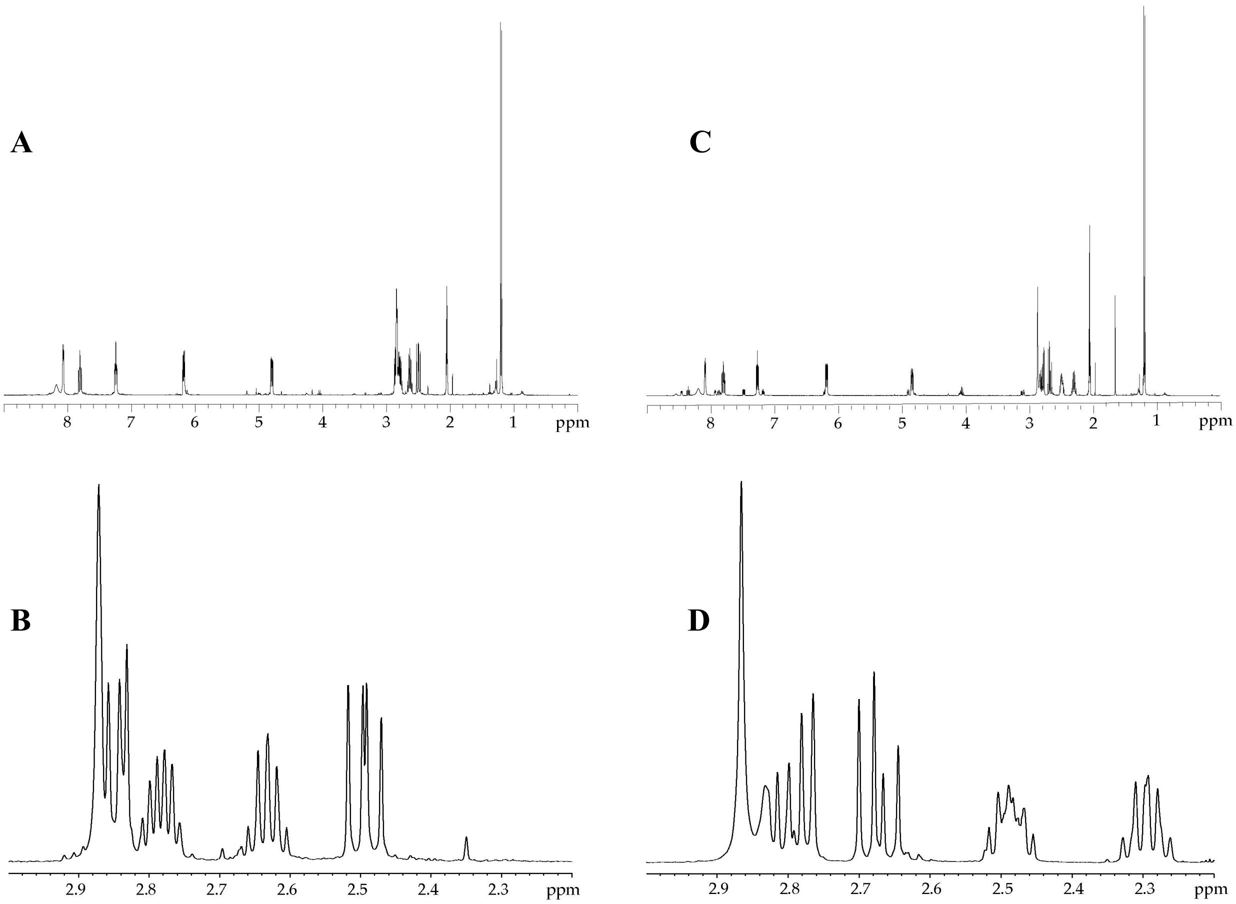

XIV. ^{1}H NMR spectra of major and minor diasteromers **8a** and **8b** in acetone-d_6. (**A**) pure **8a**; (**B**) expansion of methylene region of (**A**); (**C**) pure **8b**; and (**D**) expansion of methylene region of (**C**).

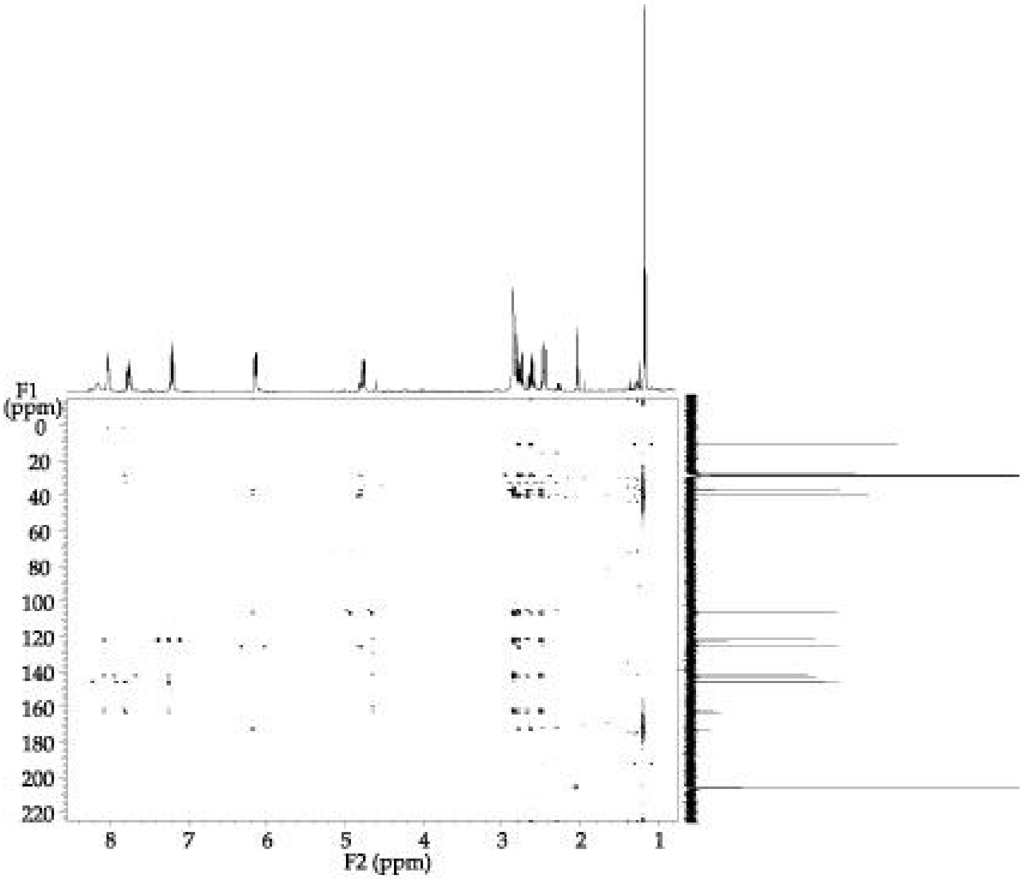

XV. [^{1}H,^{13}C]HMBC NMR spectrum revealing long range ^{1}H-^{13}C heteronuclear correlation in a 3:1 mixture of diastereomer **8a** and **8b** in acetone-d_6.

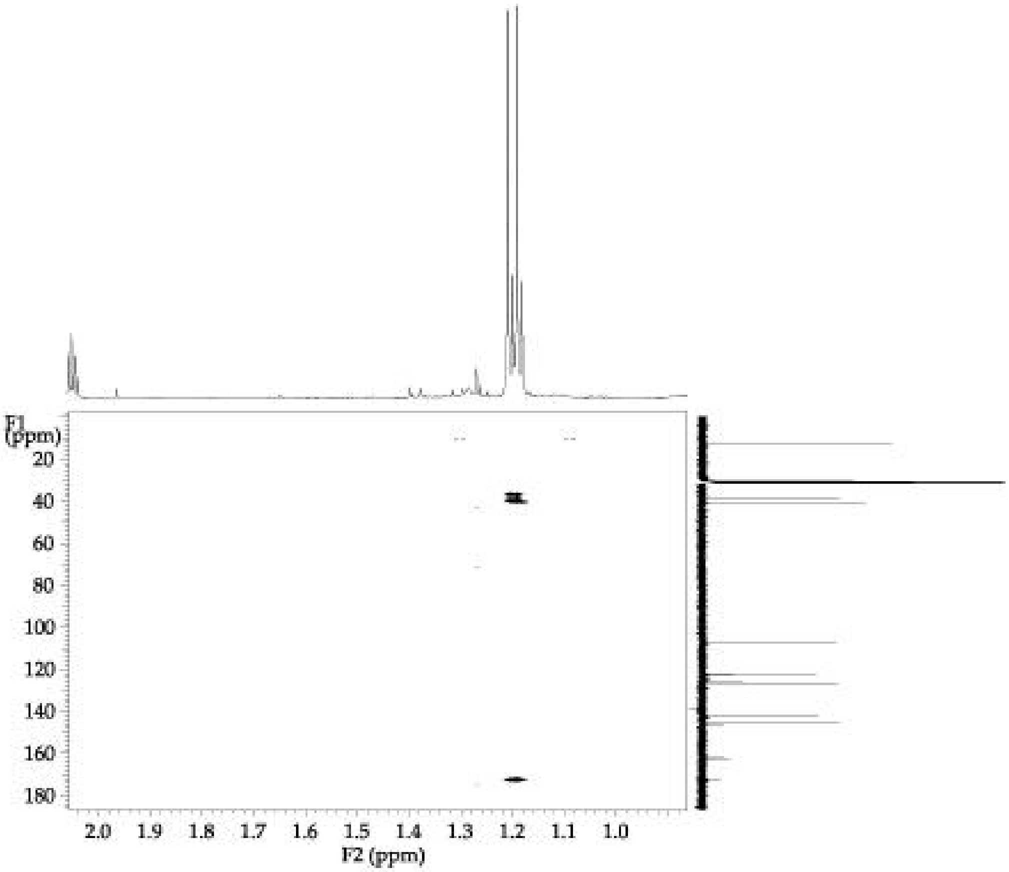

XVI. [^{1}H,^{13}C]HMBC NMR spectrum revealing long range ^{1}H-^{13}C heteronuclear correlation in a 3:1 mixture of diastereomer **8a** and **8b** in acetone- *d*$_6$. ^{1}H dimension zoomed in on methyl region to highlight lack of ^{1}H methyl-^{13}C vinyl long range correlation.

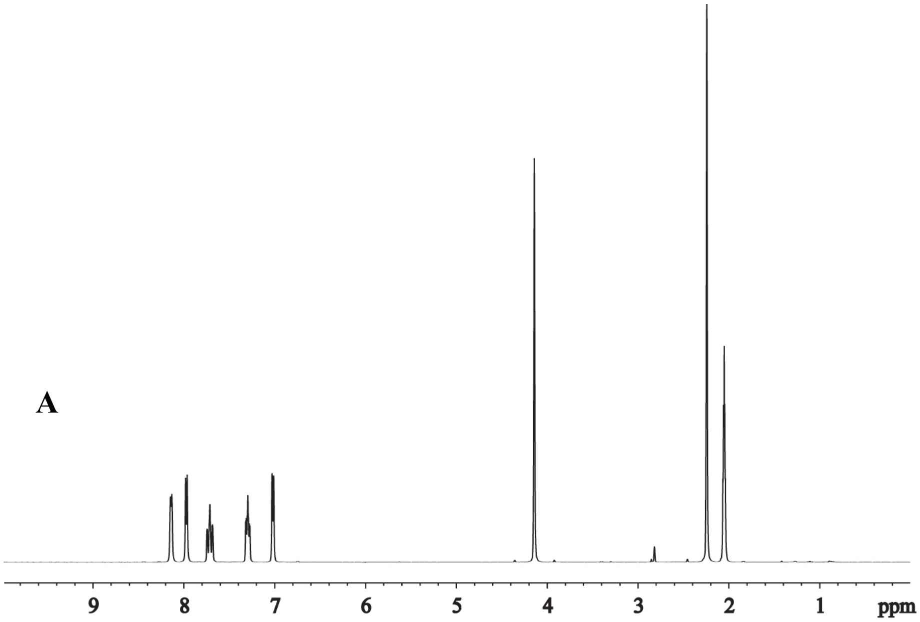

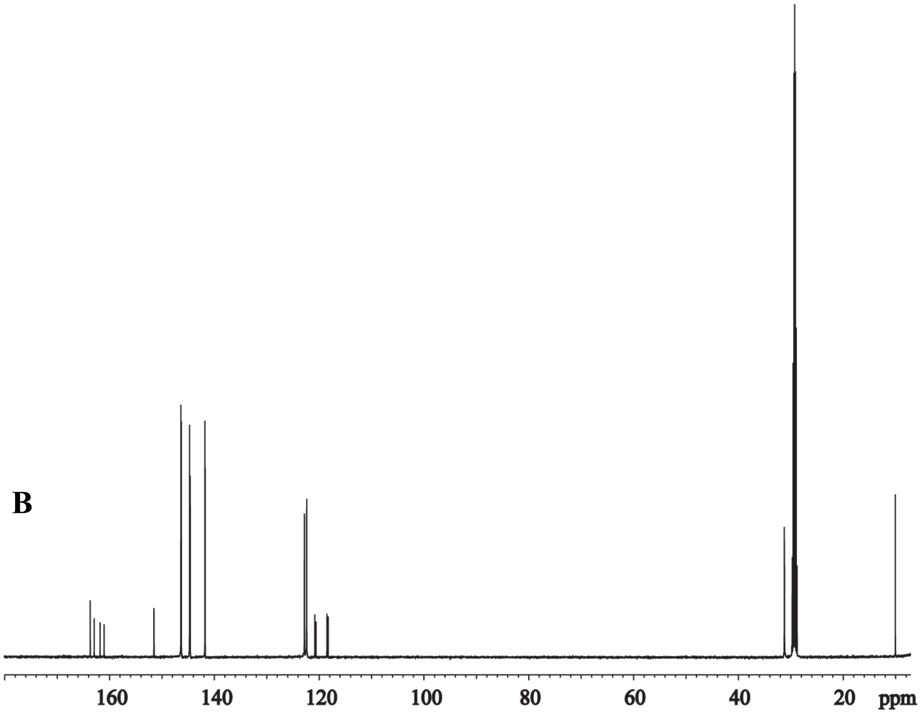

XVII. NMR spectra of aromatized 1,4-dimer **9** in acetone-d_6: (**A**) ^{1}H spectrum; and (**B**) ^{13}C spectrum.

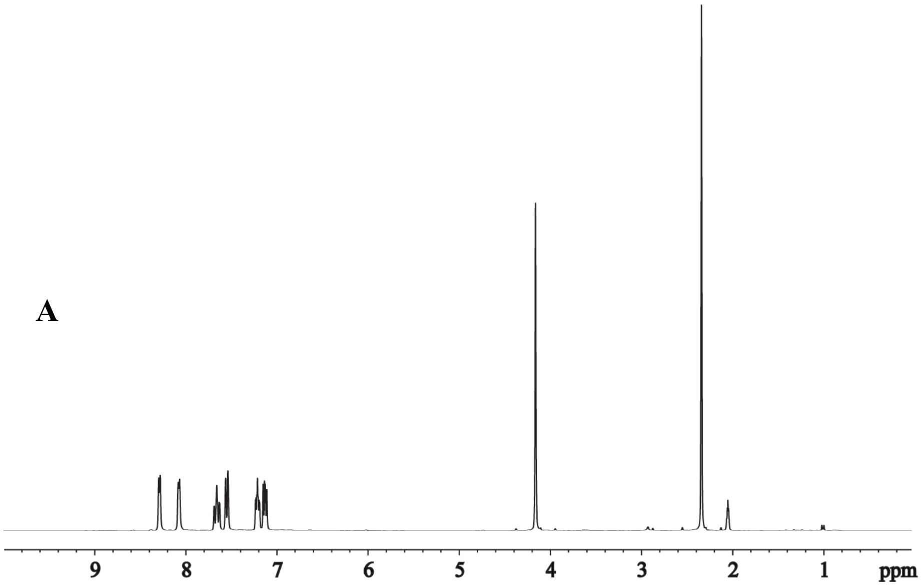

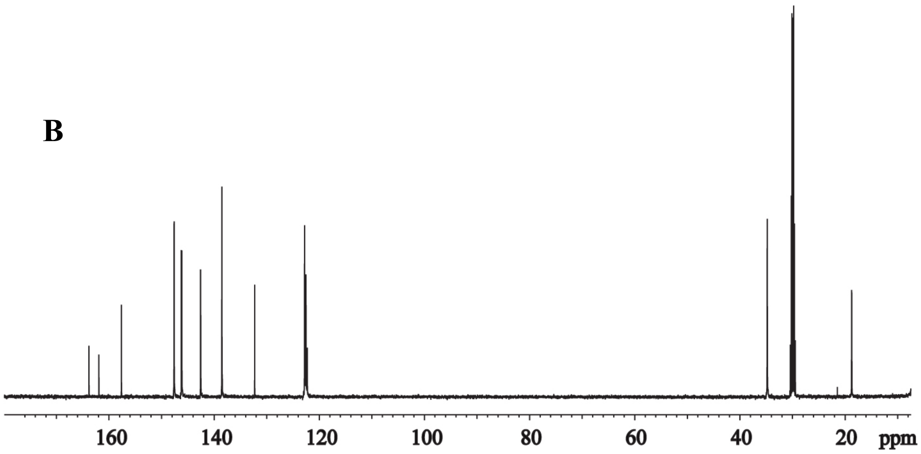

XVIII. NMR spectra of **10** in acetone-d_6: (**A**) ^{1}H spectrum; and (**B**) ^{13}C spectrum.

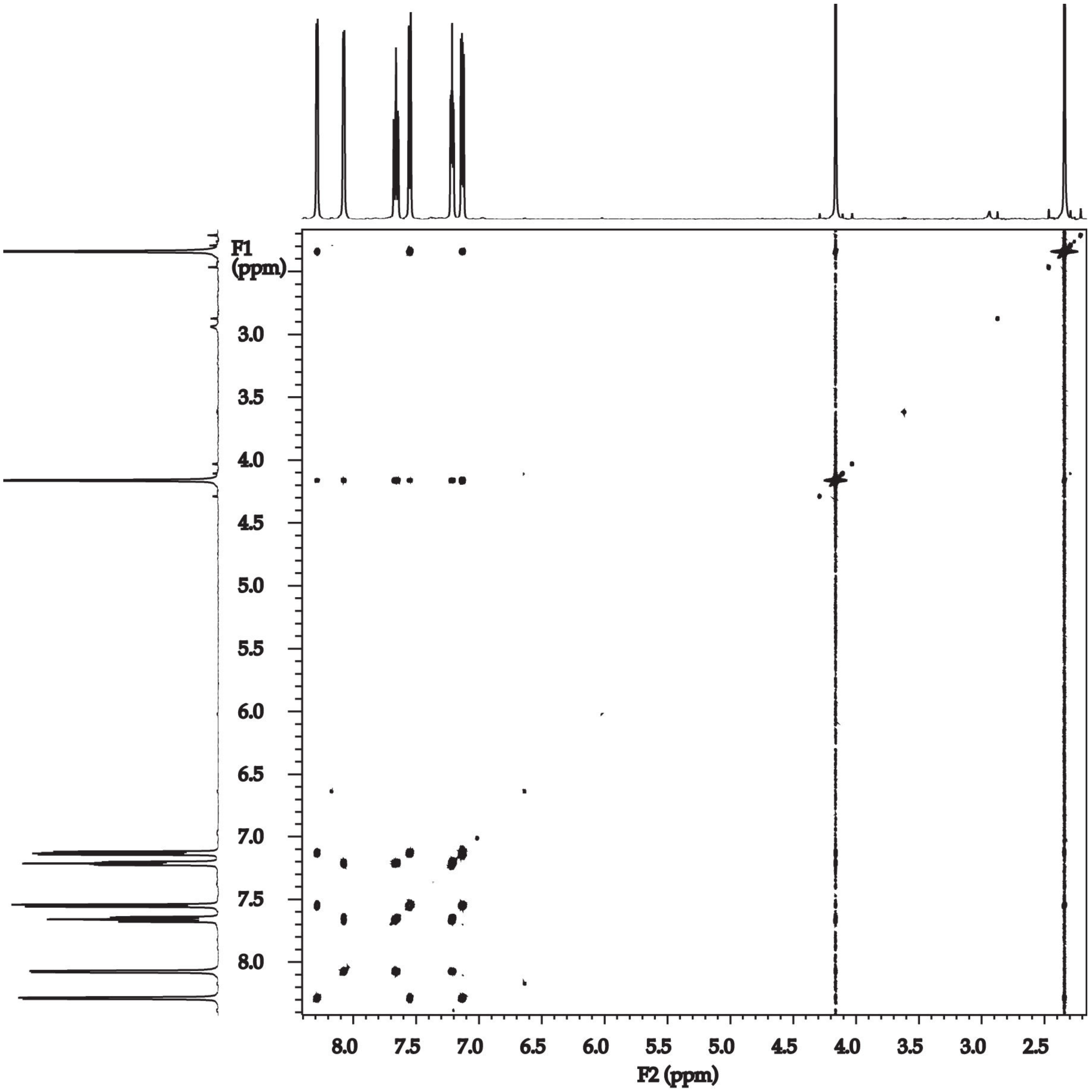

XIX. [^{1}H,^{1}H]COSY NMR spectrum of **10** recorded in acetone-d_6 at 20 ºC.

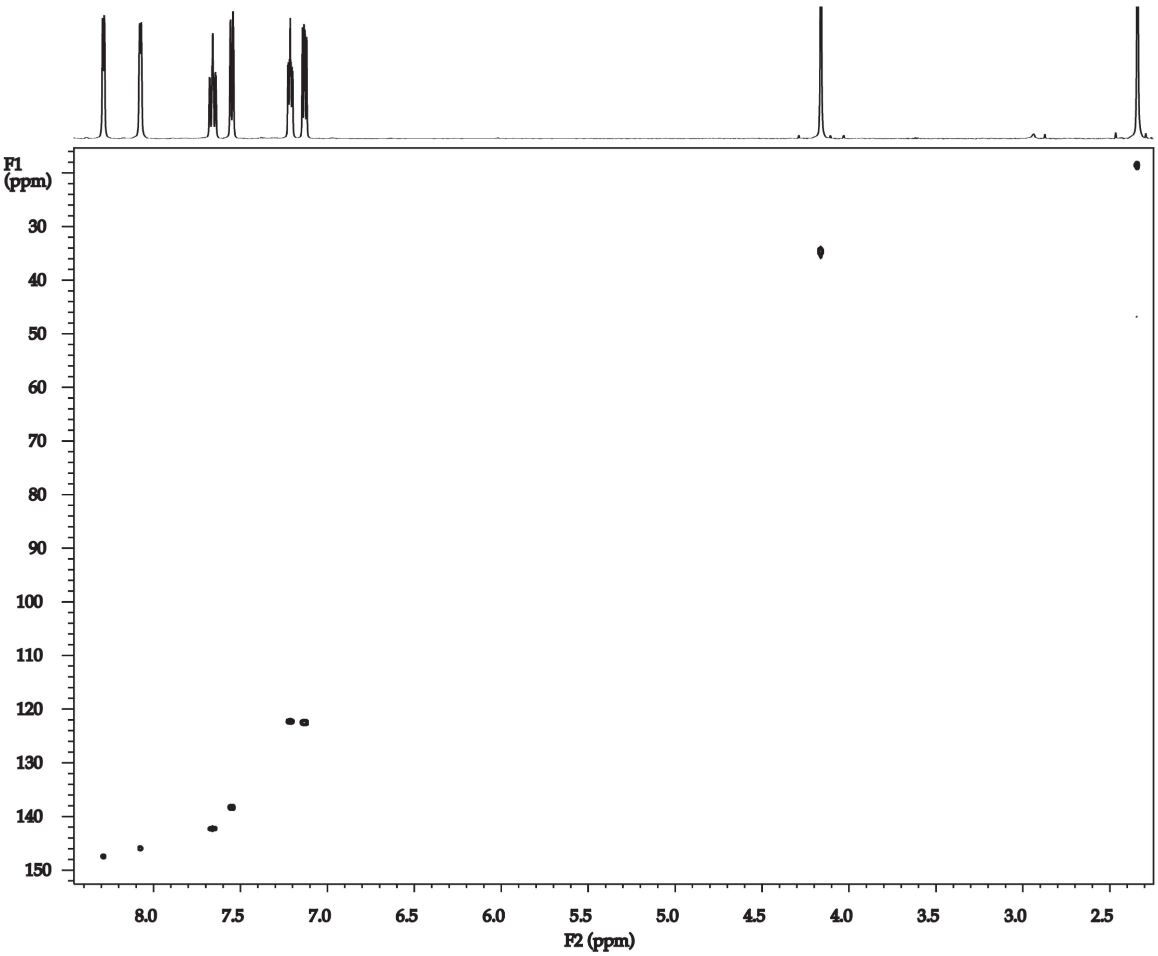

XX. [^{1}H,^{13}C]HSQC NMR spectrum of **10** recorded in acetone-d_6 at 20 ºC.

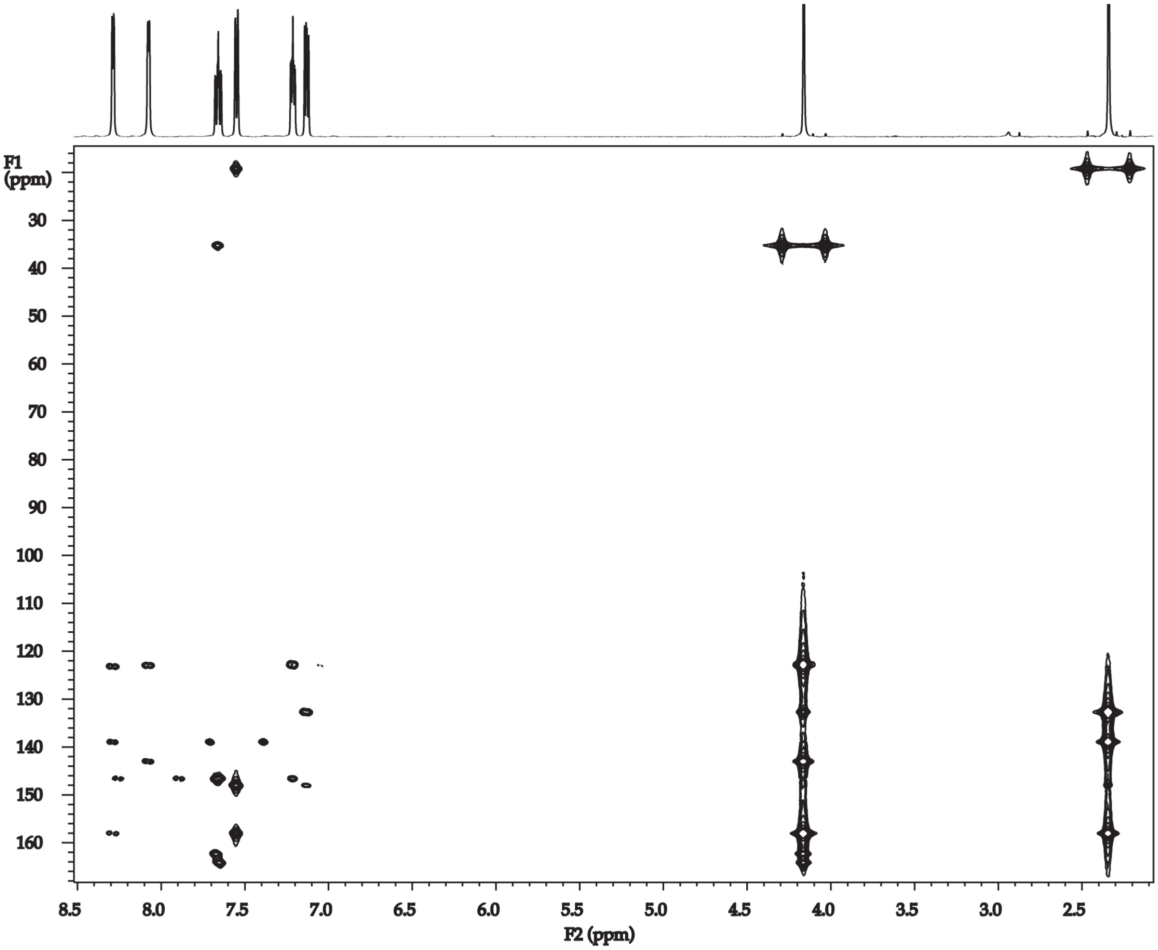

XXI. [^{1}H,^{13}C]HMBC NMR spectrum of **10** recorded in acetone-d_6 at 20 ºC.

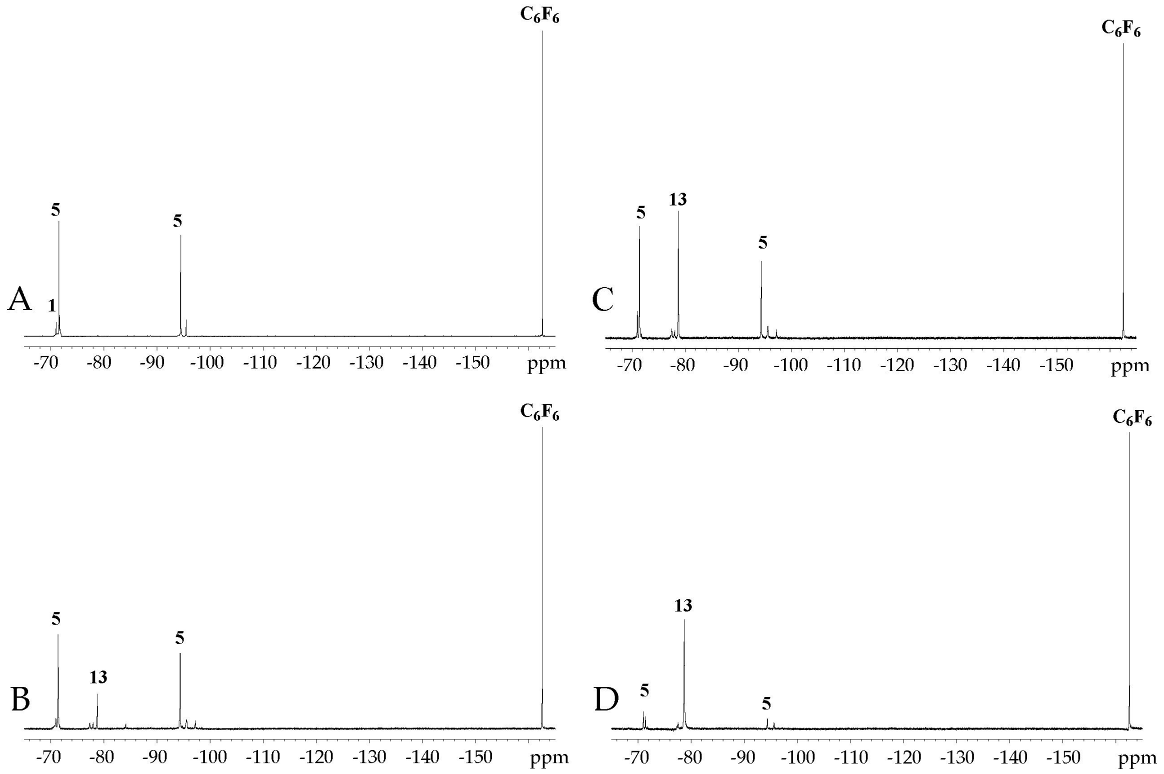

XXII. ^{19}F NMR spectra of 0.10 M **1** with 0.10 M LDA in neat THF at –78 ºC showing reaction to form **5** and **13**. (**A**) Before aging; (**B**) after aging at 0 ºC for 1 min; (**C**) after aging at 0 ºC for 3 min; and (**D**) after aging at 0 ºC for 15 min.

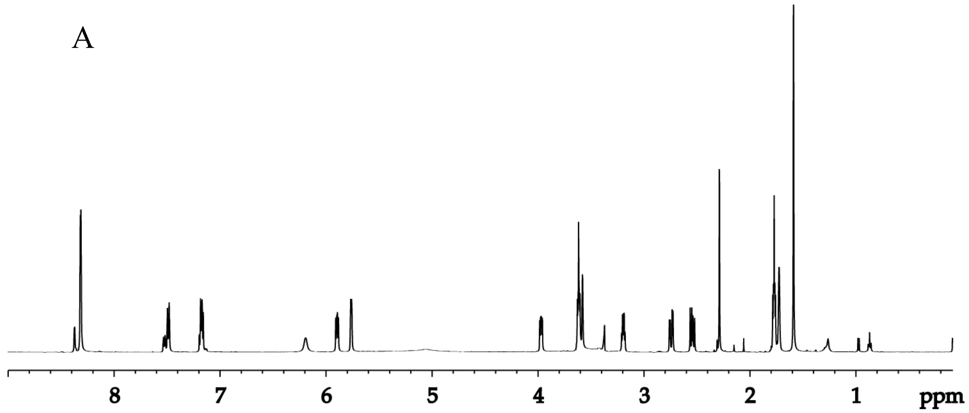

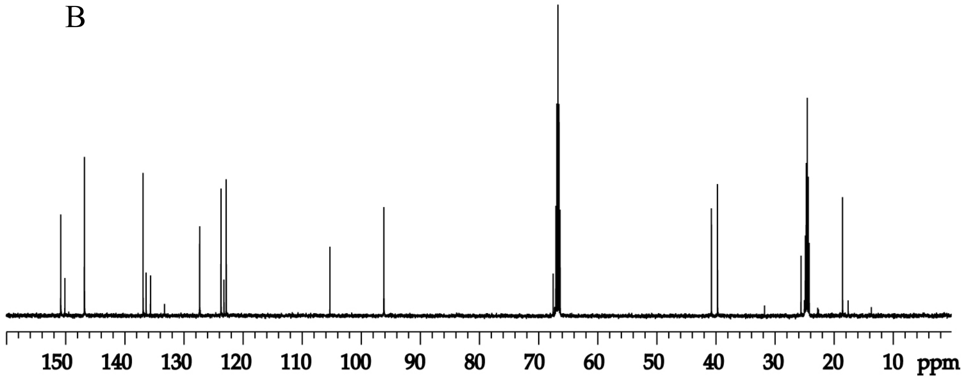

XXIII. (A) ^{1}H NMR spectrum of **23** was recorded in THF-d_8 after 30 min aging at –40 ºC; and (**B**) ^{13}C NMR spectrum of **23** was recorded in THF-d_8 after 30 min aging at –40 ºC.

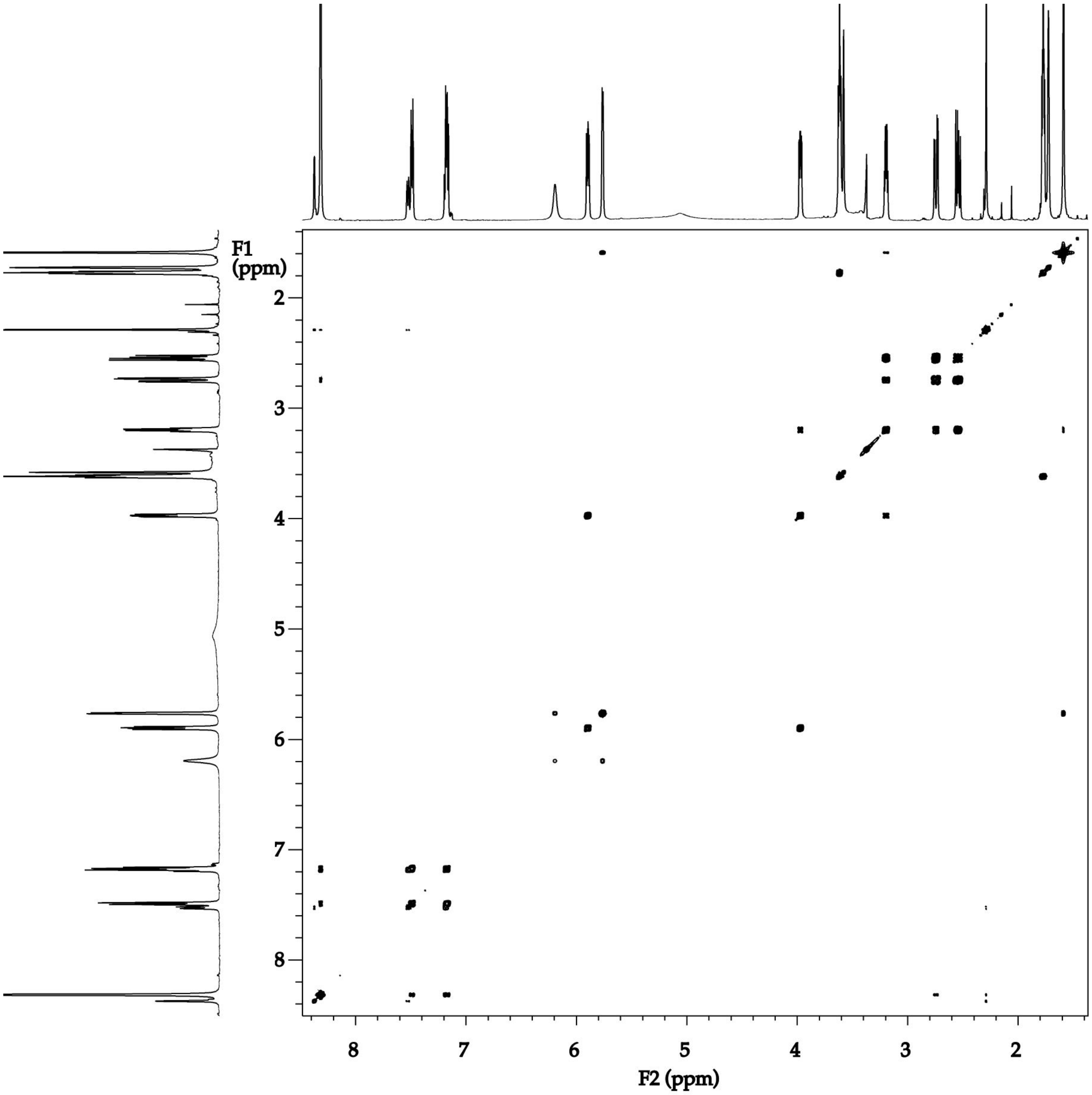

XXIV. [^{1}H,^{1}H]COSY NMR spectrum of **23** recorded in neat THF-d_8 at 20 °C.

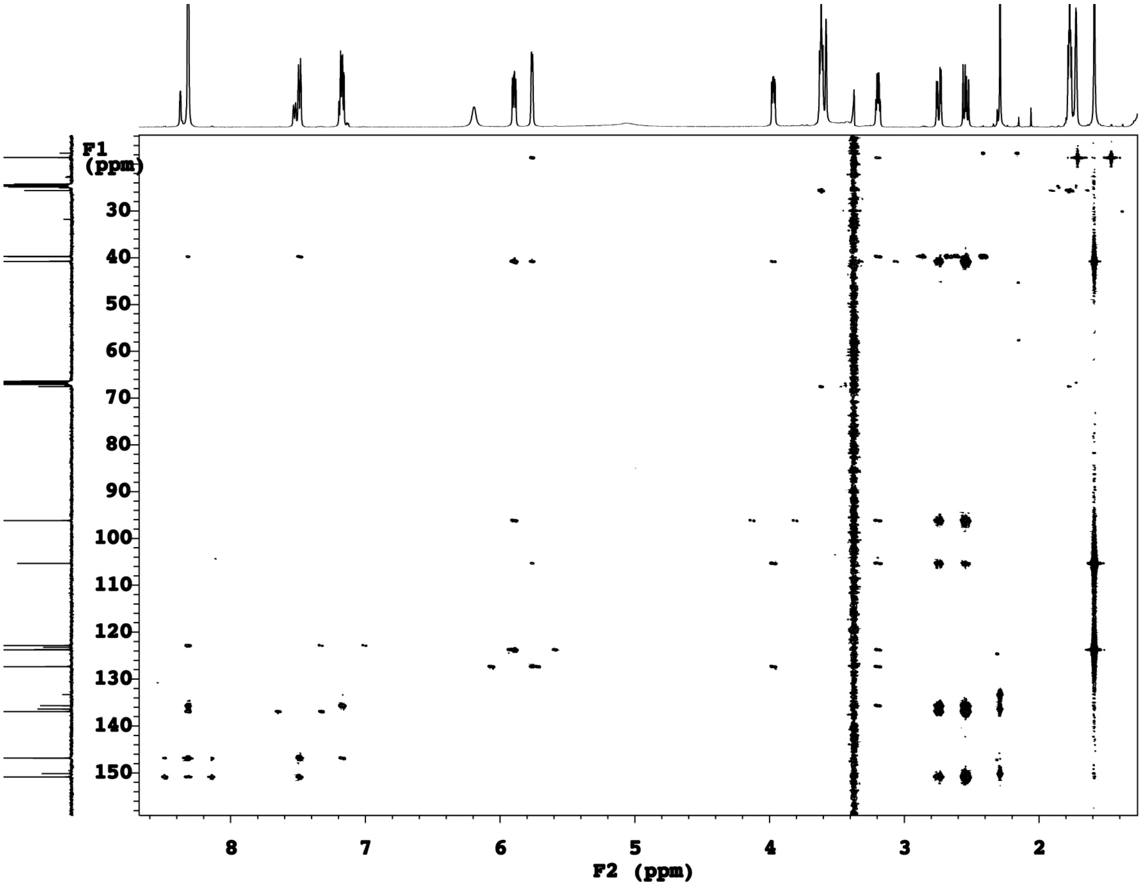

XXV. [^{1}H,^{13}C]HMBC NMR spectrum of **23** recorded in neat THF-d_8 at 20 °C.

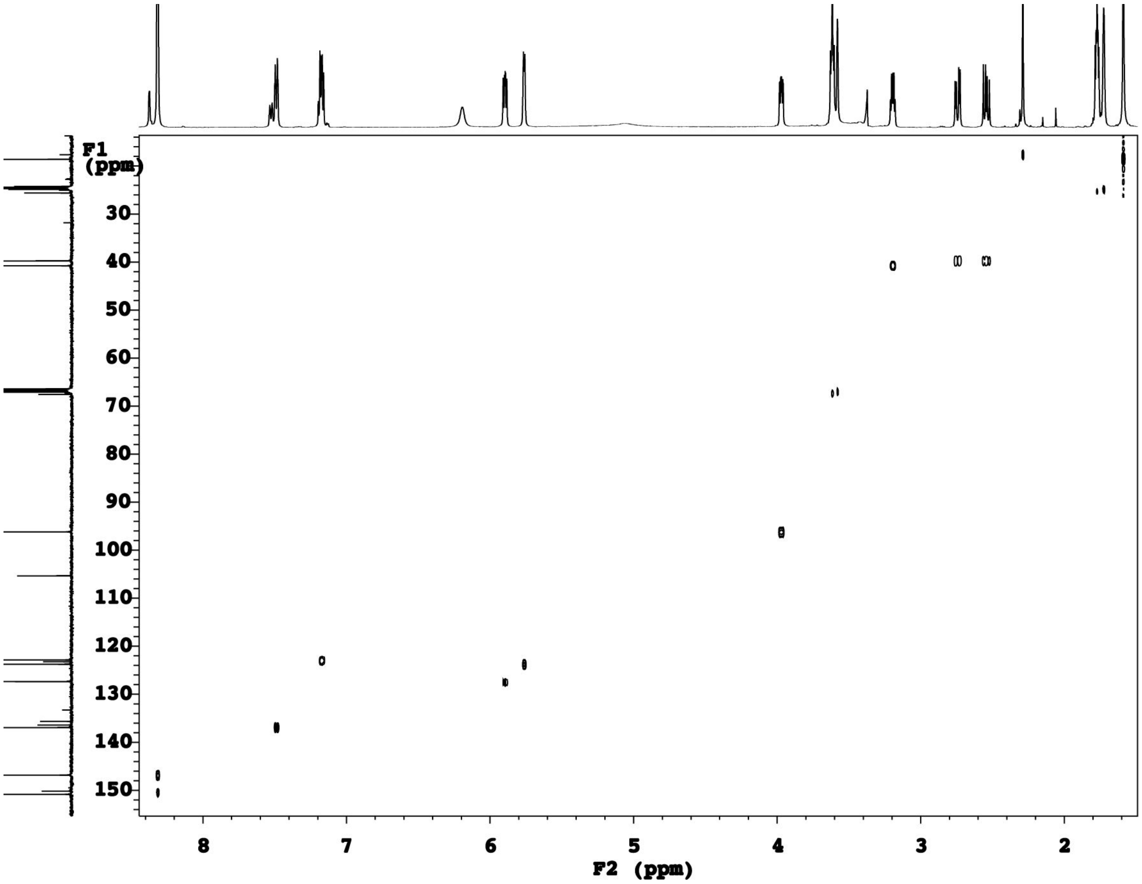

XXVI. [^{1}H,^{13}C]HSQC NMR spectrum of **23** recorded in neat THF-d_8 at 20 °C

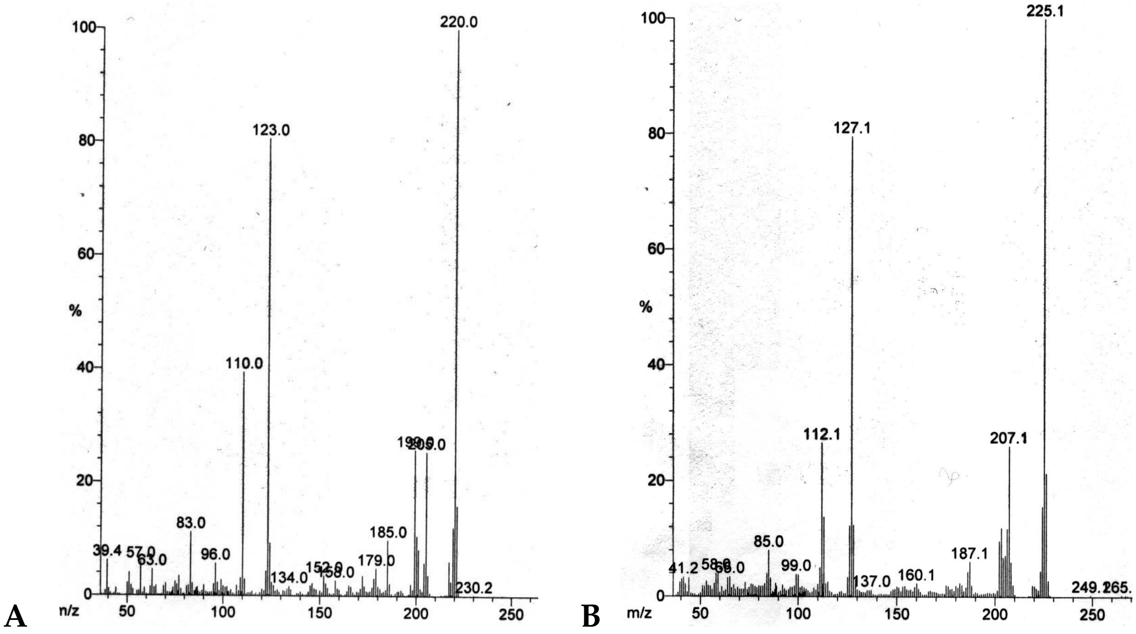

XXVII. Mass spectra of (**A**) **9**; and (**B**) **9**-d_5.

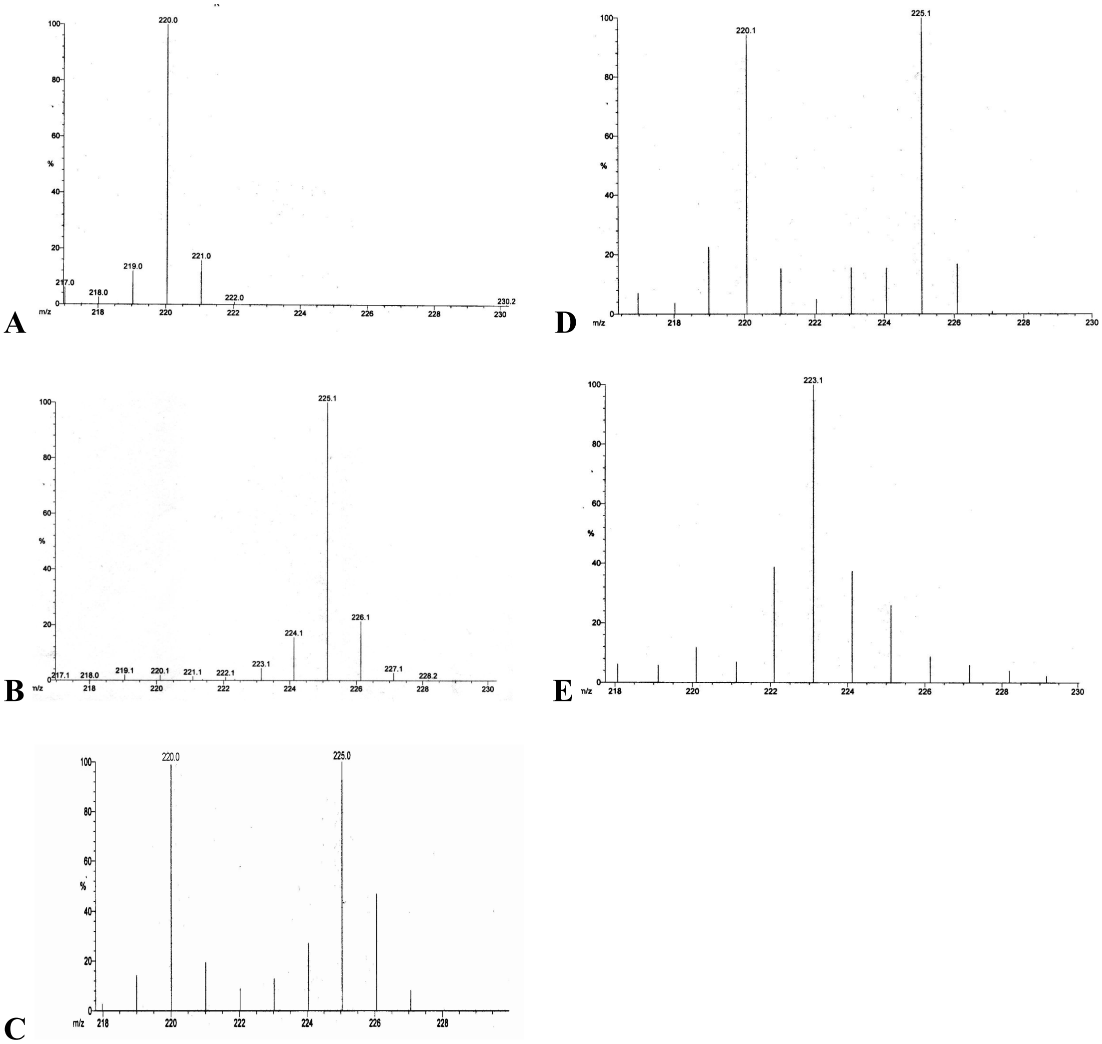

XXVIII. Expasion of M+ peak region of mass spectra. (**A**) **9**-d_0; (**B**) **9**-d_5; (**C**) **9**-d_0 and **9**-d_5 resulting from quench of independently prepared solutions of **5**-d_0 and **5**-d_5 mixed together and aged at -78 °C for 7 min; (**D**) **9**-d_0 and **9**-d_5 resulting from quench of independently prepared solutions of **5**-d_0 and **5**-d_5 mixed together and aged at -78 °C for 1.5 min; and (**E**) **9**-d_0 and **9**-d_5 resulting from quench of independently prepared solutions of **5**-d_0 and **5**-d_5 mixed together and aged at -40 °C for 60 min.

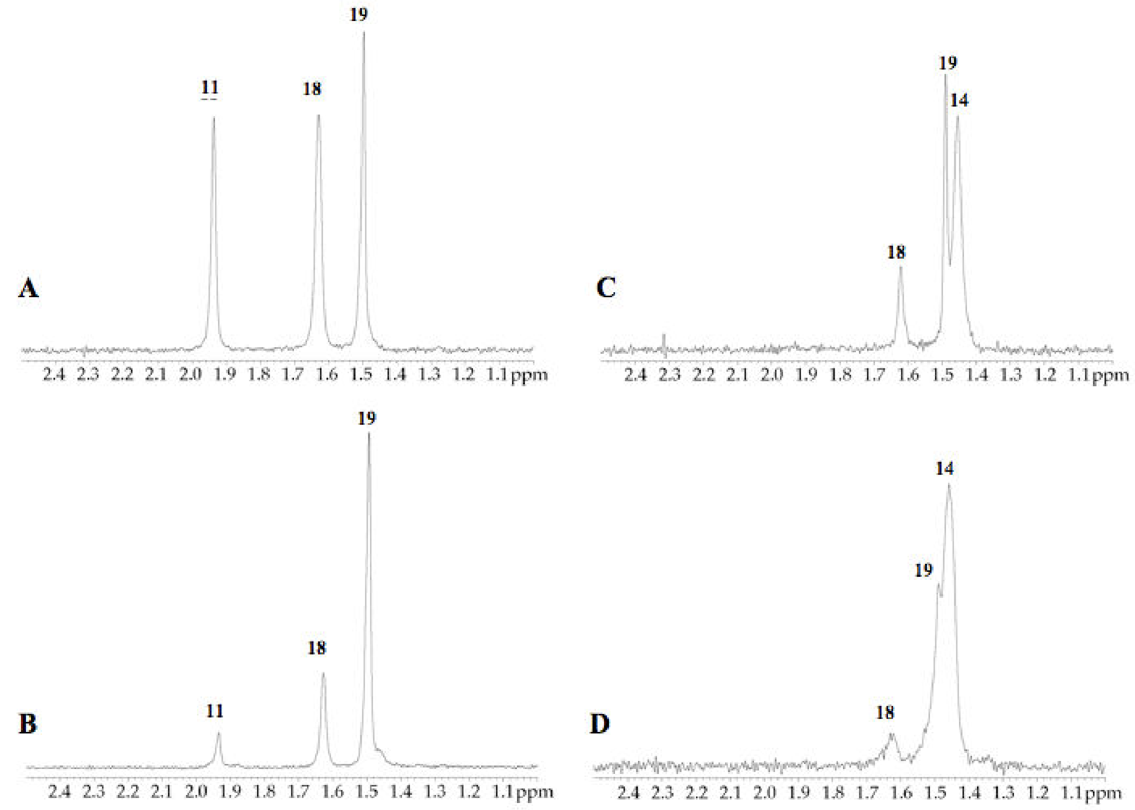

XXIX. ^{6}Li NMR spectra of 0.20 M **6** in neat THF. (**A**) Recorded at –90 ºC after addition of 0.20 M PhCN to 0.20 M ^{6}Li LDA and 2 hours aging at -90 ºC; (**B**) recorded at –90 ºC after 1 hr aging at –60 ºC; (**C**) recorded at –90 ºC after 4 min aging at –40 ºC; and (**D**) recorded at –90 ºC after 4 hours aging at –40 ºC.

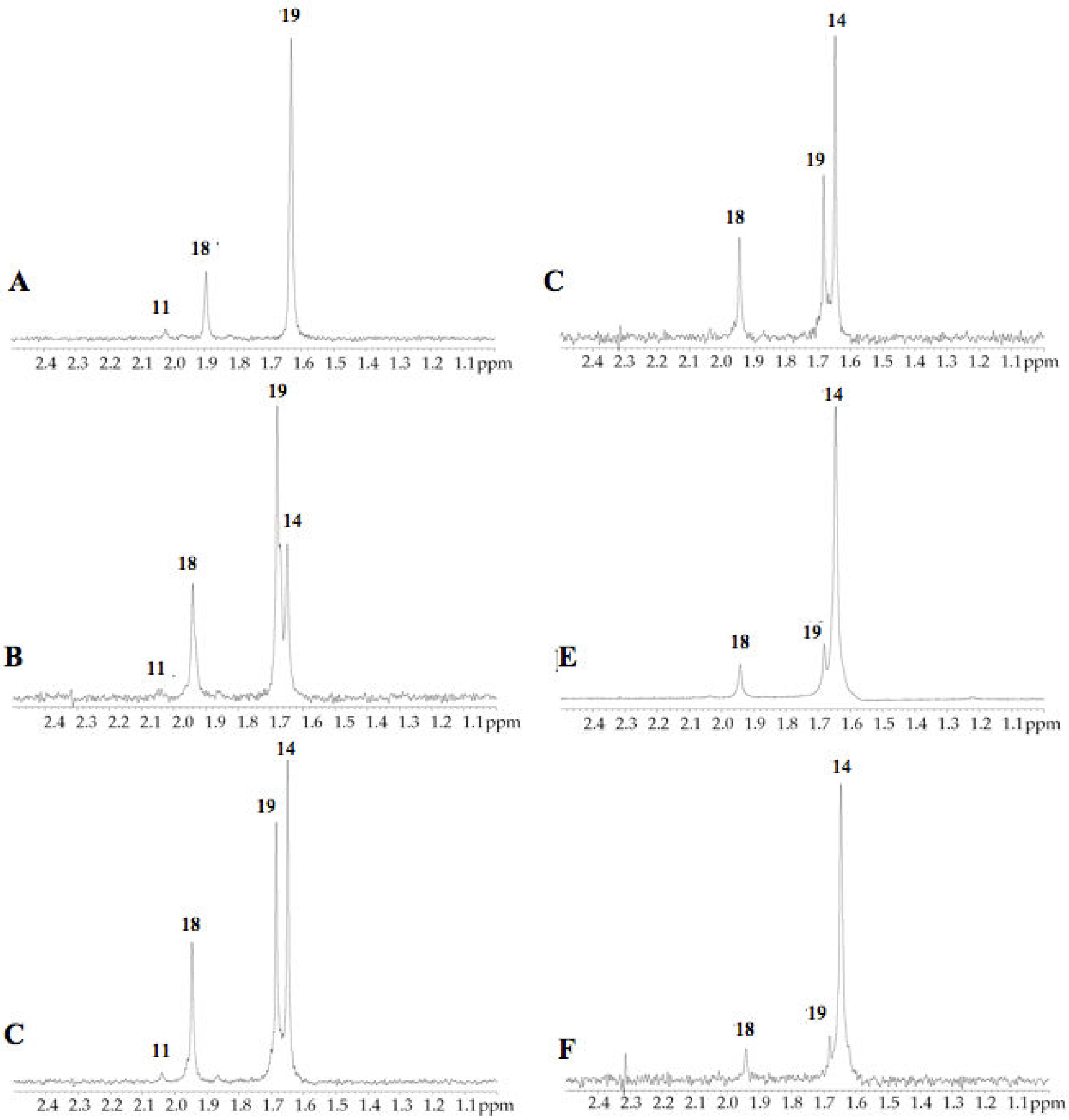

XXX. ^{6}Li NMR spectra of 0.20 M **6** in neat THF. (**A**) Recorded at –50 ºC; (**B**) recorded at –40 ºC after 4 min aging at –40 ºC; (**C**) recorded at –40 ºC after 8 min aging at –40 ºC; (**D**) recorded at –40 ºC after 12 min aging at –40 ºC; (**E**) recorded at –40 ºC after 25 min aging at –40 ºC; and (**F**) recorded at –40 ºC after 30 min aging at –40 ºC.

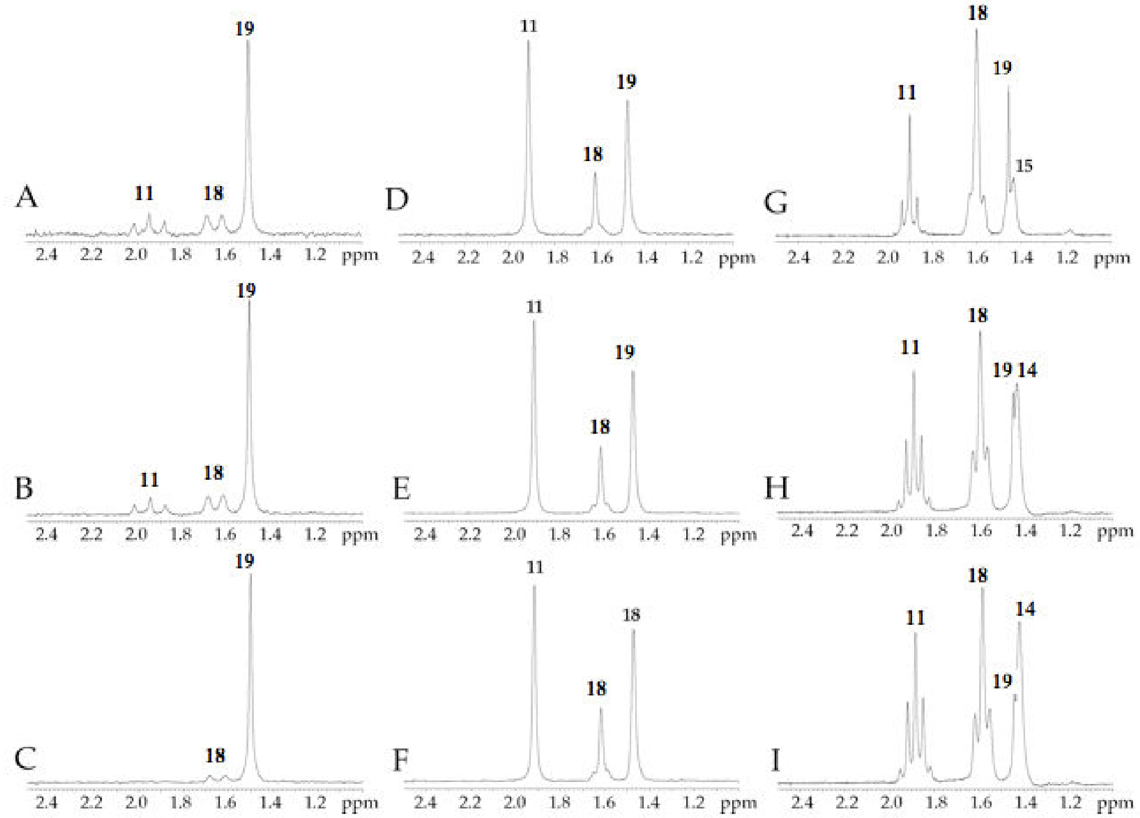

XXXI. ^{6}Li NMR spectra of 0.20 M [^{6}Li,^{15}N]LDA plus 0.26 M PhCN in neat THF at –90 ºC. After (**A**) 5 min at -78 ºC and 9 min at -90 ºC; (**B**) 3 additional min at -90 ºC; (**C**) 27 additional min at -90 ºC; (**D**) 4 min after addition of 0.20 M [^{6}Li]LDA; (**E**) 13 min after addition; (**F**)18 min after addition; (**G**) warming to -40 °C for 9 min; (**H**) warming to -40 °C for 49 min; and (**I**) warming to -40 °C for 110 min.

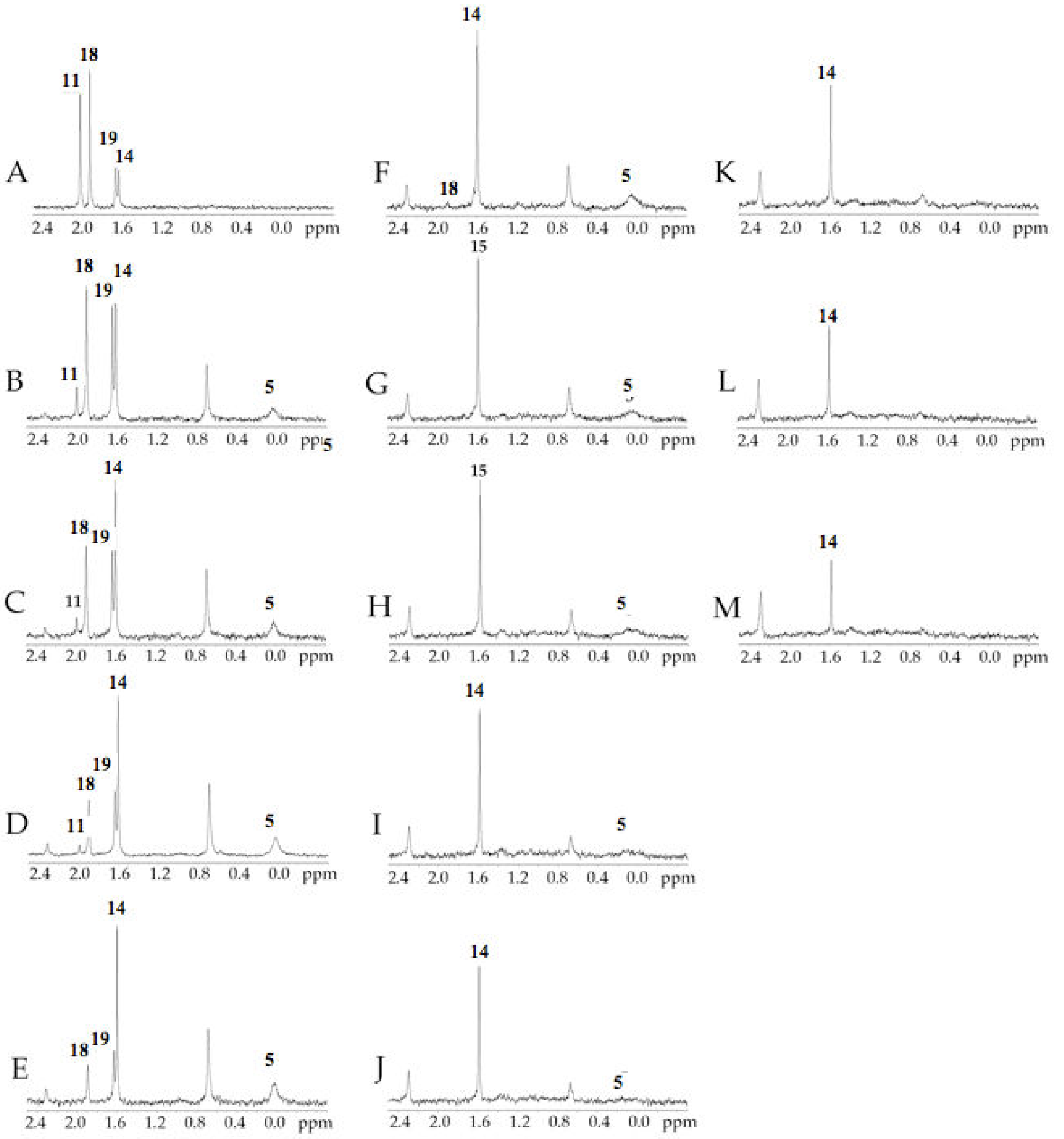

XXXII. ^{6}Li spectra of 0.10 M **6** and 0.10 M [^{6}Li]LDA in neat THF recorded at -40 °C showing reaction with 1.0 eq **1**. (**A**) Before addition of **1**; after (**B**) 8 min reaction; (**C)** 16 min reaction; (**D**) 35 min reaction; (**E**) 45 min reaction; (**F**) after 73 min reaction; (**G**) 101 min reaction; (**H**) 129 min reaction; (**I**) 157 min reaction; (J) 185 min reaction; (**K**) 241 min reaction; (**E**) 353 min reaction; and (**E**) 465 min reaction.

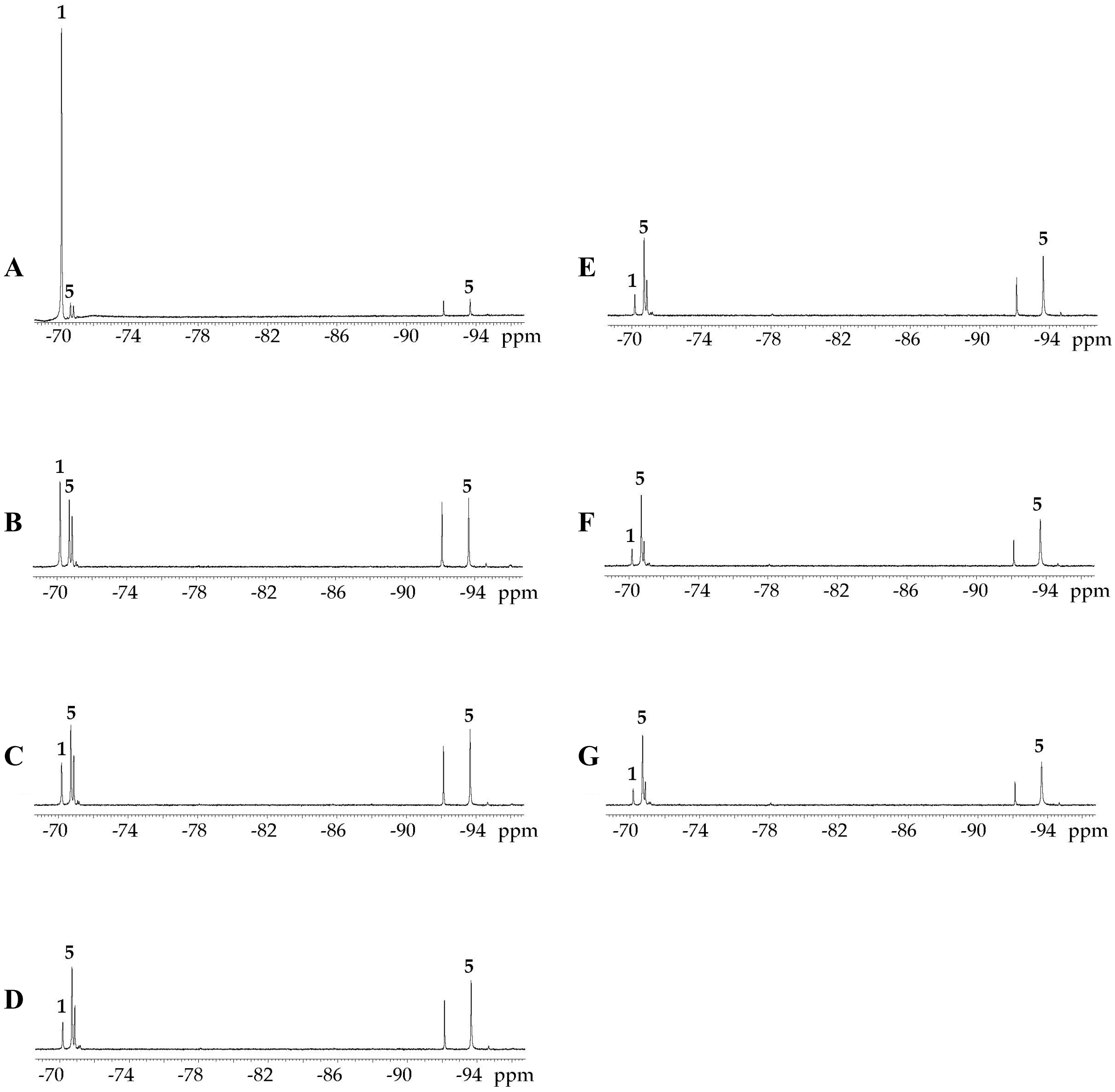

XXXIII. ^{19}F NMR spectra of 0.10 M **6** with 0.10 M LDA in neat THF at –40 ºC showing reaction with 1.0 equivof **1**. After (**A**) 20 seconds reaction; (**B**) 16 min reaction; (**C**)32 min reaction; (**D**) 49.1 min reaction; (**E**) 65 min reaction; (**F**) 98 min reaction; and (**G**) 108 min reaction.

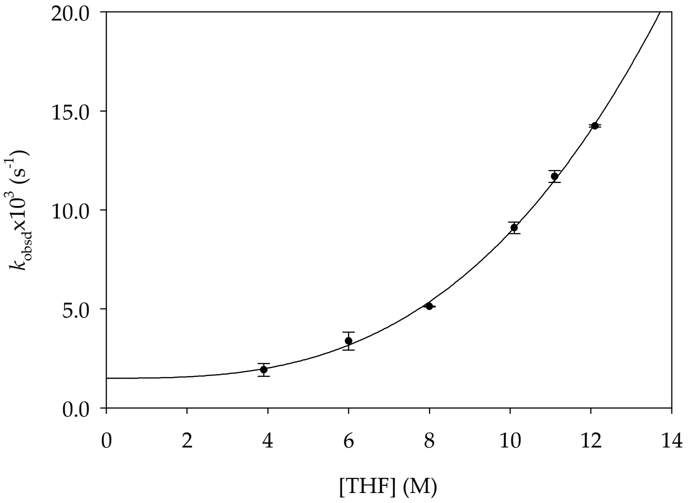

XXXIV. Plot of k_{obsd} vs [THF] in pentane for the deprotonation of 2-fluoro-3-methylpyridine (**1**, 0.01 M) by LDA (0.20 M) as determined by following loss of **1** at -20 °C by ^{19}F NMR. The curve depicts an unweighted least-squares fit to $k_{obsd} = a + k[\text{THF}]^n$ ($a = 1.50 \pm 0.28$, $k = (9.08 \pm 4.36)\times10^{-3}$, $n = 2.91 \pm 0.19$).

[THF] (M)	k_{obsd}1 (s^{-1})	k_{obsd}2 (s^{-1})	k_{obsd}avg (s^{-1})
3.9	0.00169 ± 3E-5	0.00215 ± 2E-5	0.00192 ± 3E-4
6.0	0.00304 ± 5E-5	0.00369 ± 3E-5	0.00337 ± 5E-4
8.0	0.00511 ± 9E-5	0.00513 ± 6E-5	0.00512 ± 2E-5
10.1	0.00889 ± 2E-4	0.00930 ± 4E-5	0.00909 ± 3E-4
11.1	0.0115 ± 4E-4	0.0119 ± 2E-4	0.0117 ± 3E-4
12.1	0.0142 ± 1E-3	0.0143 ± 1E-3	0.0142 ± 6E-5

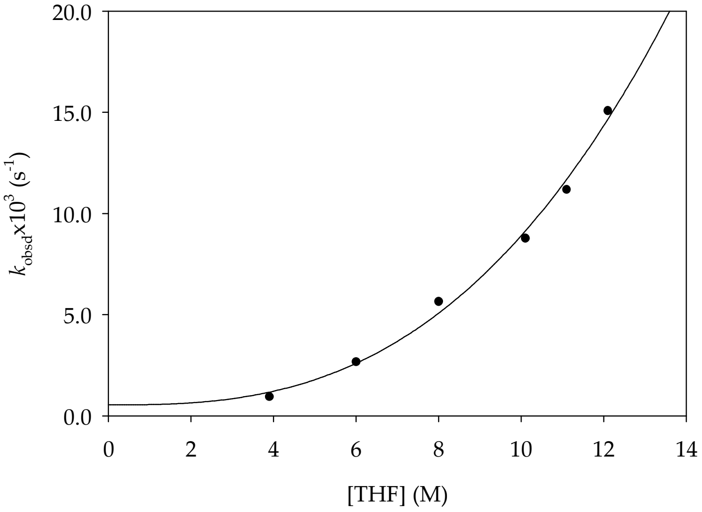

XXXV. Plot of k_{obsd} vs [THF] in 2,2,5,5-tetramethyltetrahydrofuran for the deprotonation of 2-fluoro-3-methylpyridine (**1**, 0.01 M) by LDA (0.20 M) as determined by following loss of **1** at -20 °C. The curve depicts an unweighted least-squares fit to $k_{obsd} = a + k[THF]^n$ ($a = 0.541 \pm 0.757$, $k = 0.0150 \pm 0.0163$, $n = 2.75 \pm 0.43$).

[THF] (M)	k_{obsd} (s^{-1})
3.9	0.000948 ± 5E-6
6.0	0.00267 ± 4E-5
8.0	0.00565 ± 7E-5
10.1	0.00877 ± 1E-4
11.1	0.0112 ± 2E-4
12.1	0.0151 ± 5E-4

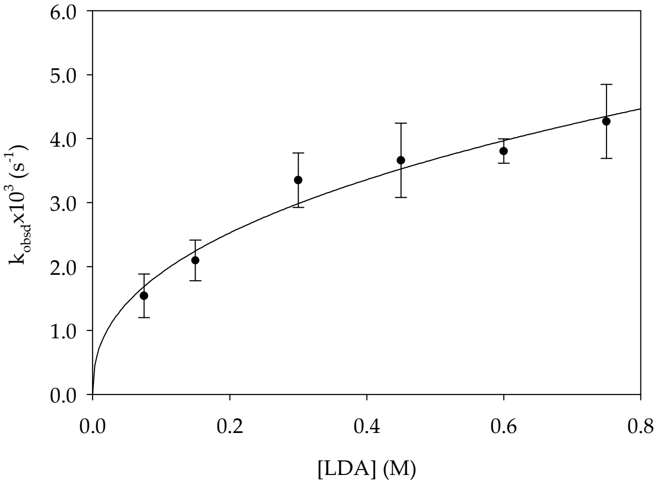

XXXVI. Plot of k_{obsd} vs [LDA] in 4.1 M THF/pentane for the deprotonation of 2-fluoro-3-methylpyridine (**1**, 0.01 M) by LDA as determined by following loss of **1**at -20 °C by ^{19}F NMR. The curve depicts an unweighted least-squares fit to $k_{obsd} = k[LDA]^n$ ($k = 4.90 \pm 0.24$, $n = 0.41 \pm 0.05$).

[LDA] (M)	$k_{obsd}1$ (s^{-1})	$k_{obsd}2$ (s^{-1})	$k_{obsd}avg$ (s^{-1})
0.075	0.00130 ± 1E-5	0.00178 ± 2E-5	0.00154 ± 3E-4
0.15	0.00187 ± 2E-5	0.00232 ± 3E-5	0.00210 ± 3E-4
0.30	0.00305 ± 3E-5	0.00365 ± 3E-5	0.00335 ± 4E-4
0.45	0.00325 ± 3E-5	0.00407 ± 4E-5	0.00366 ± 6E-4
0.60	0.00394 ± 5E-5	0.00367 ± 6E-5	0.00381 ± 2E-4
0.75	0.00468 ± 6E-5	0.00386 ± 6E-5	0.00427 ± 6E-4

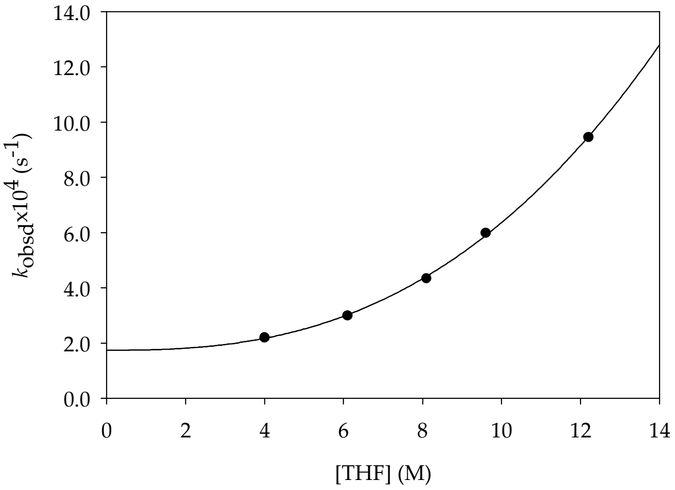

XXXVII. Plot of k_{obsd} vs [THF] in pentane for the deprotonation of 2-fluoro-3-methylpyridine (**1**, 0.01 M) by LDA (0.20 M) as determined by following formation of **5** at -40 °C via in situ IR. The curve depicts an unweighted least-squares fit to $k_{obsd} = a + k[\mathrm{THF}]^n$ ($a = 1.75 \pm 0.13$, $k = (0.012 \pm 0.003)$, $n = 2.59 \pm 0.11$).

[THF] (M)	k_{obsd} (s^{-1})
4.0	0.000220 ± 6E-6
6.1	0.000300 ± 1E-6
8.1	0.000435 ± 9E-6
9.6	0.000599 ± 4E-5
12.2	0.000946 ± 5E-5

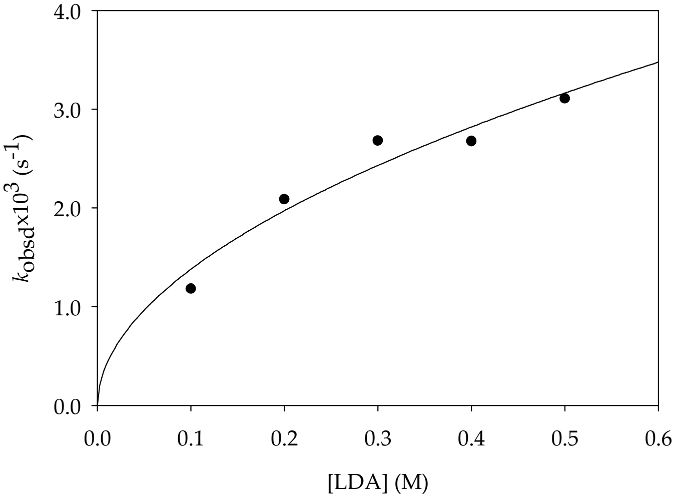

XXXVIII. Plot of k_{obsd} vs [LDA] in 12.3 M THF for the deprotonation of 2-fluoro-3-methylpyridine (**1**, 0.01 M) by LDA as determined by following product formation at -40 °C via in situ IR. The curve depicts an unweighted least-squares fit to $k_{obsd} = k[LDA]^n$ ($k = (4.53 \pm 0.47)\times10^{-3}$, $n = 0.52 \pm 0.09$).

[LDA] (M)	k_{obsd} (s^{-1})
0.10	0.00118 ± 7E-5
0.20	0.00209 ± 2E-4
0.30	0.00268 ± 2E-4
0.40	0.00268 ± 2E-4
0.50	0.00311 ± 3E-4

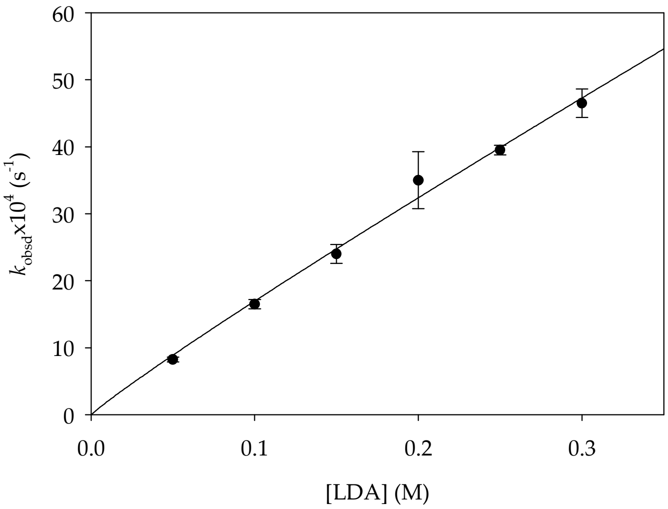

XXXIX. Plot of k_{obsd} vs [LDA] in 10.0 M THF/pentane for the condensation of PhCN (0.01 M) by LDA as determined by following loss of starting material at -78 °C via in situ IR. The curve depicts an unweighted least-squares fit to $k_{obsd} = k[\mathrm{LDA}]^n$ ($k = 1.45 \pm 0.24$, $n = 0.93 \pm 0.05$).

[LDA] (M)	k_{obsd}1 (s^{-1})	k_{obsd}2 (s^{-1})	k_{obsd}avg (s^{-1})
0.05	0.00085 ± 2E-5	0.00080 ± 1E-5	0.00083 ± 9E-5
0.10	0.0017 ± 1E-4	0.0016 ± 1E-4	0.00165 ± 1E-4
0.15	0.0023 ± 1E-4	0.0025 ± 2E-4	0.0024 ± 1E-4
0.20	0.0038 ± 2E-4	0.0032 ± 3E-4	0.0035 ± 2E-4
0.25	0.0039 ± 1E-4	0.0040 ± 1E-4	0.00395 ± 7E-5
0.30	0.0045 ± 2E-4	0.0048 ± 2E-4	0.00465 ± 8E-5

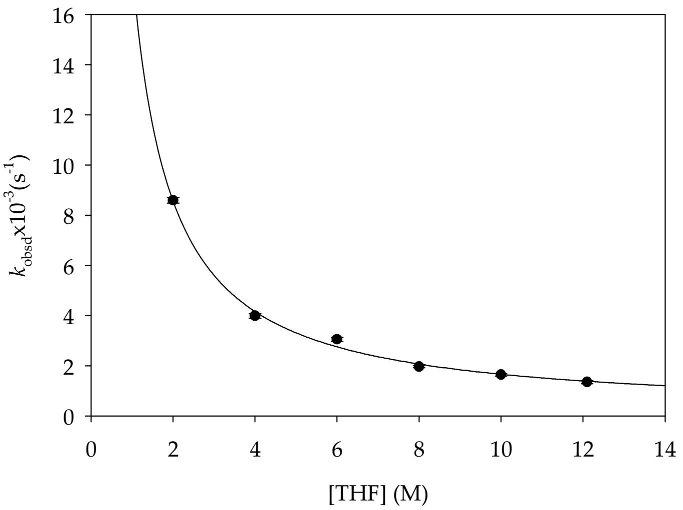

L. Plot of k_{obsd} vs [THF] in pentane for the the condensation of PhCN (0.01 M) by LDA (0.20 M) as determined by following product formation at -78 °C via in situ IR. The curve depicts an unweighted least-squares fit to $k_{\text{obsd}} = a + k[\text{THF}]^n$ ($a = 1.76 \pm 0.5$, $k = 0.16 \pm 0.26$, $n = -1.07 \pm 0.07$).

[THF] (M)	$k_{\text{obsd}}1$ (s^{-1})	$k_{\text{obsd}}2$ (s^{-1})	k_{obsd}avg (s^{-1})
2.0	0.0085 ± 3E-4	0.0087 ± 2E-4	0.0086 ± 2E-4
4.0	0.0041 ± 4E-4	0.0039 ± 3E-4	0.0040 ± 1E-4
6.0	0.0031 ± 2E-4	0.0030 ± 1E-4	0.0031 ± 1E-4
8.0	0.0019 ± 1E-4	0.0020 ± 2E-4	0.00195 ± 1E-4
10.0	0.0017 ± 1E-4	0.0016 ± 4E-4	0.00165 ± 7E-5
12.1	0.0013 ± 3E-4	0.0014 ± 3E-4	0.00135 ± 9E-5

XLI. X-Ray structure of **9**.

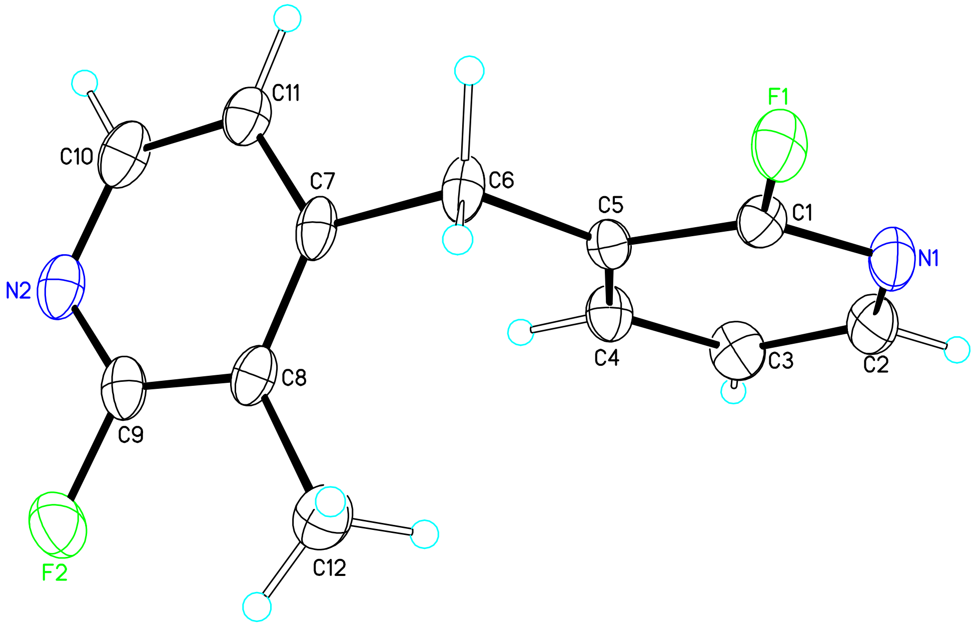

Table 1. Crystal data and structure refinement.

Identification code	**9**	
Empirical formula	C12 H10 F2 N2	
Formula weight	220.22	
Temperature	173(2) K	
Wavelength	0.71073 Å	
Crystal system	Triclinic	
Space group	P-1	
Unit cell dimensions	a = 7.3370(8) Å	α= 92.050(4)°.
	b = 10.6664(11) Å	β= 95.711(4)°.
	c = 13.1655(14) Å	γ = 94.074(4)°.
Volume	1021.67(19) $Å^3$	
Z	4	
Density (calculated)	1.432 Mg/m^3	
Absorption coefficient	0.112 mm^{-1}	
F(000)	456	
Crystal size	0.50 x 0.45 x 0.40 mm^3	
Theta range for data collection	1.56 to 28.49°.	
Index ranges	-9<=h<=9, -14<=k<=13, -17<=l<=17	
Reflections collected	21945	
Independent reflections	5007 [R(int) = 0.0339]	
Completeness to theta = 28.49°	96.7 %	
Absorption correction	Semi-empirical from equivalents	
Max. and min. transmission	0.9565 and 0.9461	
Refinement method	Full-matrix least-squares on F^2	
Data / restraints / parameters	5007 / 0 / 291	
Goodness-of-fit on F^2	1.513	
Final R indices [I>2sigma(I)]	R1 = 0.0767, wR2 = 0.2157	
R indices (all data)	R1 = 0.1012, wR2 = 0.2301	
Largest diff. peak and hole	0.743 and -0.316 e.$Å^{-3}$	

Table 2. Atomic coordinates (x 10^4) and equivalent isotropic displacement parameters ($\AA^2$x 10^3) U(eq) is defined as one third of the trace of the orthogonalized U^{ij} tensor.

	x	y	z	U(eq)
F(1)	1209(1)	1264(1)	8718(1)	33(1)
F(2)	4831(2)	6726(1)	6081(1)	42(1)
F(3)	1972(1)	1148(1)	6266(1)	38(1)
F(4)	-1560(2)	-4333(1)	9015(1)	47(1)
N(1)	3972(2)	505(1)	8843(1)	32(1)
N(2)	4775(2)	7376(1)	7706(1)	33(1)
N(3)	-842(2)	1829(1)	5982(1)	34(1)
N(4)	-1502(2)	-4951(1)	7390(1)	32(1)
C(1)	3050(2)	1482(2)	8695(1)	24(1)
C(2)	5790(3)	694(2)	8810(1)	36(1)
C(3)	6639(2)	1850(2)	8624(1)	34(1)
C(4)	5564(2)	2858(2)	8467(1)	28(1)
C(5)	3691(2)	2710(1)	8506(1)	22(1)
C(6)	2371(2)	3720(1)	8362(1)	28(1)
C(7)	3247(2)	4981(1)	8124(1)	26(1)
C(8)	3699(2)	5217(2)	7153(1)	26(1)
C(9)	4428(2)	6445(2)	7027(1)	29(1)
C(10)	4350(2)	7095(2)	8645(2)	35(1)
C(11)	3595(2)	5943(2)	8894(1)	30(1)
C(12)	3432(3)	4257(2)	6284(1)	36(1)
C(13)	137(2)	895(2)	6236(1)	25(1)
C(14)	-2666(3)	1594(2)	5952(1)	38(1)
C(15)	-3479(2)	451(2)	6172(1)	35(1)
C(16)	-2361(2)	-512(2)	6439(1)	29(1)
C(17)	-490(2)	-306(1)	6479(1)	21(1)
C(18)	872(2)	-1271(1)	6756(1)	26(1)
C(19)	-2(2)	-2542(2)	6992(1)	25(1)
C(20)	-438(2)	-2793(2)	7963(1)	27(1)
C(21)	-1159(2)	-4031(2)	8074(1)	29(1)
C(22)	-1087(2)	-4654(2)	6451(1)	33(1)
C(23)	-342(2)	-3496(2)	6212(1)	27(1)
C(24)	-192(3)	-1867(2)	8844(2)	42(1)

Table 3. Bond lengths [Å] and angles [°].

F(1)-C(1)	1.3577(18)
F(2)-C(9)	1.347(2)
F(3)-C(13)	1.3504(18)
F(4)-C(21)	1.347(2)
N(1)-C(1)	1.292(2)
N(1)-C(2)	1.340(2)
N(2)-C(9)	1.306(2)
N(2)-C(10)	1.344(2)
N(3)-C(13)	1.304(2)
N(3)-C(14)	1.340(2)
N(4)-C(21)	1.301(2)
N(4)-C(22)	1.345(2)
C(1)-C(5)	1.400(2)
C(2)-C(3)	1.383(3)
C(3)-C(4)	1.388(2)
C(4)-C(5)	1.378(2)
C(5)-C(6)	1.503(2)
C(6)-C(7)	1.506(2)
C(7)-C(8)	1.380(2)
C(7)-C(11)	1.407(2)
C(8)-C(9)	1.402(2)
C(8)-C(12)	1.495(2)
C(10)-C(11)	1.376(2)
C(13)-C(17)	1.389(2)
C(14)-C(15)	1.372(3)
C(15)-C(16)	1.393(2)
C(16)-C(17)	1.370(2)
C(17)-C(18)	1.514(2)
C(18)-C(19)	1.514(2)
C(19)-C(20)	1.379(2)
C(19)-C(23)	1.411(2)
C(20)-C(21)	1.406(2)
C(20)-C(24)	1.485(3)
C(22)-C(23)	1.375(2)
C(1)-N(1)-C(2)	115.61(14)
C(9)-N(2)-C(10)	114.15(15)
C(13)-N(3)-C(14)	115.70(15)
C(21)-N(4)-C(22)	114.15(15)
N(1)-C(1)-F(1)	114.56(13)
N(1)-C(1)-C(5)	128.80(15)
F(1)-C(1)-C(5)	116.64(13)
N(1)-C(2)-C(3)	122.73(16)
C(2)-C(3)-C(4)	118.65(16)
C(5)-C(4)-C(3)	120.53(15)

C(4)-C(5)-C(1)	113.67(14)
C(4)-C(5)-C(6)	126.10(14)
C(1)-C(5)-C(6)	120.24(14)
C(5)-C(6)-C(7)	114.32(13)
C(8)-C(7)-C(11)	119.16(15)
C(8)-C(7)-C(6)	120.77(15)
C(11)-C(7)-C(6)	120.06(16)
C(7)-C(8)-C(9)	114.86(15)
C(7)-C(8)-C(12)	123.70(15)
C(9)-C(8)-C(12)	121.44(16)
N(2)-C(9)-F(2)	114.40(14)
N(2)-C(9)-C(8)	128.84(17)
F(2)-C(9)-C(8)	116.76(15)
N(2)-C(10)-C(11)	124.38(16)
C(10)-C(11)-C(7)	118.58(17)
N(3)-C(13)-F(3)	114.99(13)
N(3)-C(13)-C(17)	127.58(15)
F(3)-C(13)-C(17)	117.44(14)
N(3)-C(14)-C(15)	123.12(17)
C(14)-C(15)-C(16)	118.58(17)
C(17)-C(16)-C(15)	119.96(16)
C(16)-C(17)-C(13)	115.06(14)
C(16)-C(17)-C(18)	125.11(14)
C(13)-C(17)-C(18)	119.82(14)
C(19)-C(18)-C(17)	114.19(13)
C(20)-C(19)-C(23)	119.36(15)
C(20)-C(19)-C(18)	121.13(15)
C(23)-C(19)-C(18)	119.49(15)
C(19)-C(20)-C(21)	114.46(15)
C(19)-C(20)-C(24)	124.74(16)
C(21)-C(20)-C(24)	120.80(17)
N(4)-C(21)-F(4)	114.08(14)
N(4)-C(21)-C(20)	129.21(17)
F(4)-C(21)-C(20)	116.71(15)
N(4)-C(22)-C(23)	124.31(16)
C(22)-C(23)-C(19)	118.48(16)

Symmetry transformations used to generate equivalent atoms:

Table 4. Anisotropic displacement parameters ($Å^2$x 10^3). The anisotropic displacement factor exponent takes the form: $-2\pi^2[h^2a^{*2}U^{11} + ... + 2 h k a^* b^* U^{12}]$

	U^{11}	U^{22}	U^{33}	U^{23}	U^{13}	U^{12}
F(1)	23(1)	24(1)	51(1)	2(1)	6(1)	-6(1)
F(2)	45(1)	38(1)	45(1)	13(1)	10(1)	2(1)
F(3)	26(1)	27(1)	60(1)	10(1)	7(1)	-9(1)
F(4)	54(1)	44(1)	46(1)	12(1)	12(1)	-2(1)
N(1)	33(1)	22(1)	42(1)	6(1)	6(1)	5(1)
N(2)	22(1)	26(1)	50(1)	5(1)	3(1)	4(1)
N(3)	39(1)	26(1)	39(1)	11(1)	8(1)	7(1)
N(4)	21(1)	29(1)	46(1)	7(1)	2(1)	4(1)
C(1)	21(1)	22(1)	28(1)	-1(1)	3(1)	0(1)
C(2)	36(1)	33(1)	44(1)	10(1)	9(1)	18(1)
C(3)	20(1)	40(1)	43(1)	8(1)	4(1)	9(1)
C(4)	23(1)	24(1)	35(1)	4(1)	2(1)	-1(1)
C(5)	21(1)	20(1)	23(1)	2(1)	1(1)	0(1)
C(6)	20(1)	17(1)	48(1)	6(1)	5(1)	2(1)
C(7)	17(1)	19(1)	43(1)	5(1)	1(1)	5(1)
C(8)	19(1)	22(1)	37(1)	0(1)	-1(1)	6(1)
C(9)	18(1)	26(1)	44(1)	9(1)	3(1)	4(1)
C(10)	27(1)	24(1)	51(1)	-6(1)	-3(1)	0(1)
C(11)	26(1)	26(1)	38(1)	1(1)	2(1)	6(1)
C(12)	36(1)	32(1)	39(1)	-2(1)	0(1)	4(1)
C(13)	26(1)	22(1)	27(1)	1(1)	6(1)	-2(1)
C(14)	39(1)	36(1)	40(1)	10(1)	6(1)	15(1)
C(15)	22(1)	41(1)	44(1)	6(1)	4(1)	7(1)
C(16)	22(1)	26(1)	39(1)	4(1)	3(1)	0(1)
C(17)	22(1)	19(1)	21(1)	-2(1)	1(1)	0(1)
C(18)	19(1)	21(1)	39(1)	5(1)	4(1)	-1(1)
C(19)	14(1)	21(1)	41(1)	5(1)	1(1)	3(1)
C(20)	21(1)	25(1)	36(1)	1(1)	1(1)	3(1)
C(21)	19(1)	28(1)	42(1)	10(1)	3(1)	1(1)
C(22)	27(1)	25(1)	44(1)	-4(1)	-3(1)	0(1)
C(23)	21(1)	23(1)	37(1)	2(1)	1(1)	0(1)
C(24)	42(1)	39(1)	44(1)	-5(1)	7(1)	4(1)

Table 5. Hydrogen coordinates (x 10^4) and isotropic displacement parameters (Å^{2}x 10^3)

	x	y	z	U(eq)
H(2)	6527	4	8919	44
H(3)	7932	1953	8605	40
H(4)	6123	3658	8332	33
H(6A)	1753	3817	8992	34
H(6B)	1416	3443	7798	34
H(10)	4586	7735	9171	42
H(11)	3314	5799	9571	36
H(12A)	4164(9)	3582(8)	6439(2)	54
H(12B)	3780(5)	4630(4)	5685(7)	54
H(12C)	2182(14)	3954(4)	6180(2)	54
H(14)	-3431	2249	5771	45
H(15)	-4778	319	6142	42
H(16)	-2895	-1311	6593	35
H(18A)	1628	-1384	6182	31
H(18B)	1705	-941	7359	31
H(22)	-1325	-5287	5918	39
H(23)	-62	-3341	5536	33
H(24A)	987(15)	-1713(3)	9041(3)	63
H(24B)	-750(7)	-2175(4)	9352(7)	63
H(24C)	-667(7)	-1164(9)	8662(3)	63